Exploring the continuum proton and neutron rich on the way to FAIR

H. Simon ● GSI Darmstadt

FUSTIPEN

… *ab initio* approaches for 2020

Caen, France

October 4th-11th, 2015

Novel Neutron Detector: NeuLAND

K. Boretzky

Fully active neutron detector based on scintillators (calorimetry & tracking)

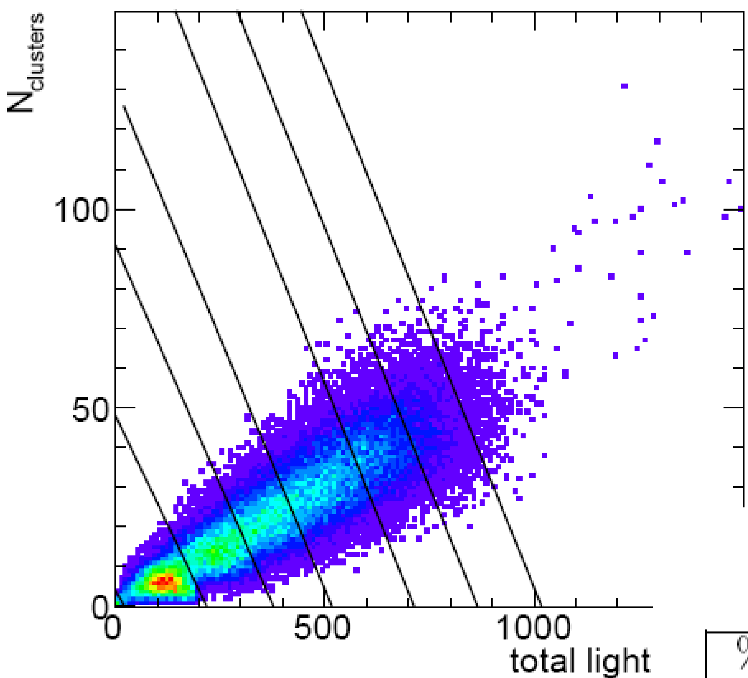

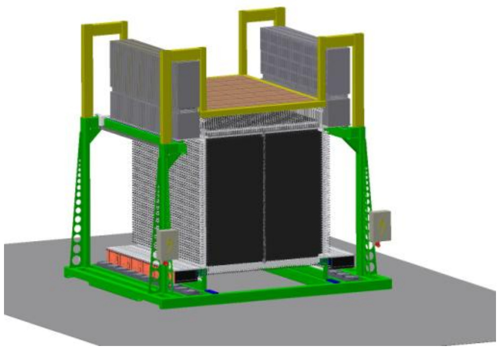

%		1000 MeV generated 1n	2n	3n	4n	5n
detected	1n	**89**	12	1	0	0
	2n	7	**78**	23	3	0
	3n	0	8	**63**	26	5
	4n	0	0	12	**63**	40
	5n	0	0	0	7	**46**
	6n	0	0	0	0	8

Previously < 50%

Previously <5% !

➔ 4/5n decay channels in reach

30 double planes
2 x 50 paddles each
5 x 5 x 250 cm³
RP408 / R8619ASSY

FPGA TDC readout

Experimental equipment on the way …

- NeuLAND demonstrator (40 cm depth with only 4 double planes and 800 readout channels) at RIKEN up to end of 2017, participation in various beam times

- at GSI continuation of production (4 more double planes ready), production scheme dominated by funding profile, 11-15 out of 30 d.p. in 2018

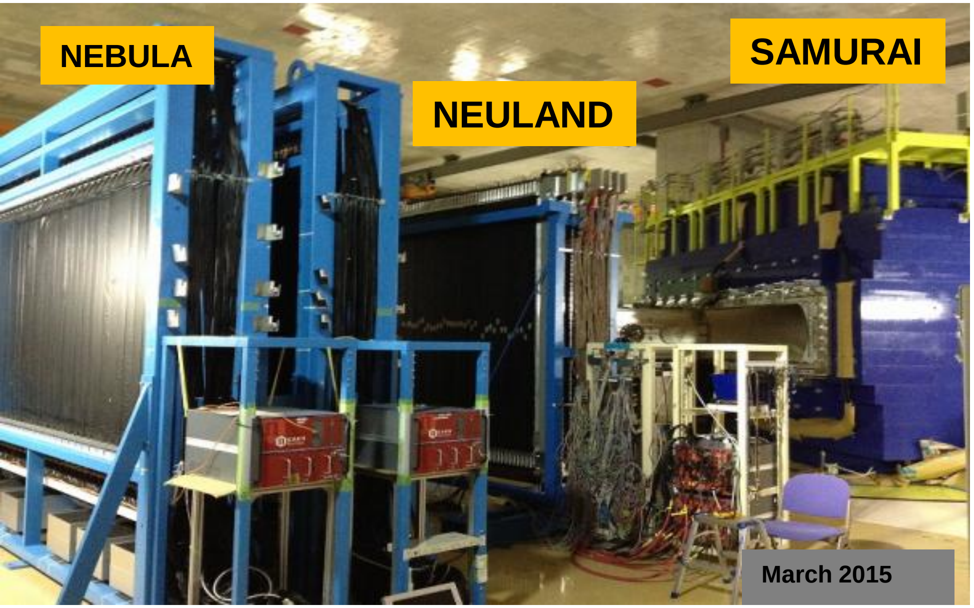

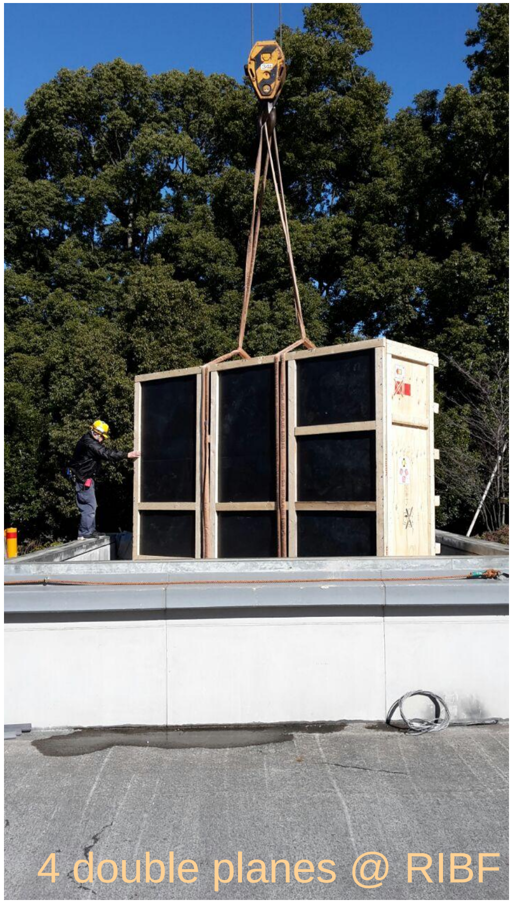

… e.g. to RIKEN
Back to GSI
Q4/2017

RIKEN: “Performance studies for the prototype”

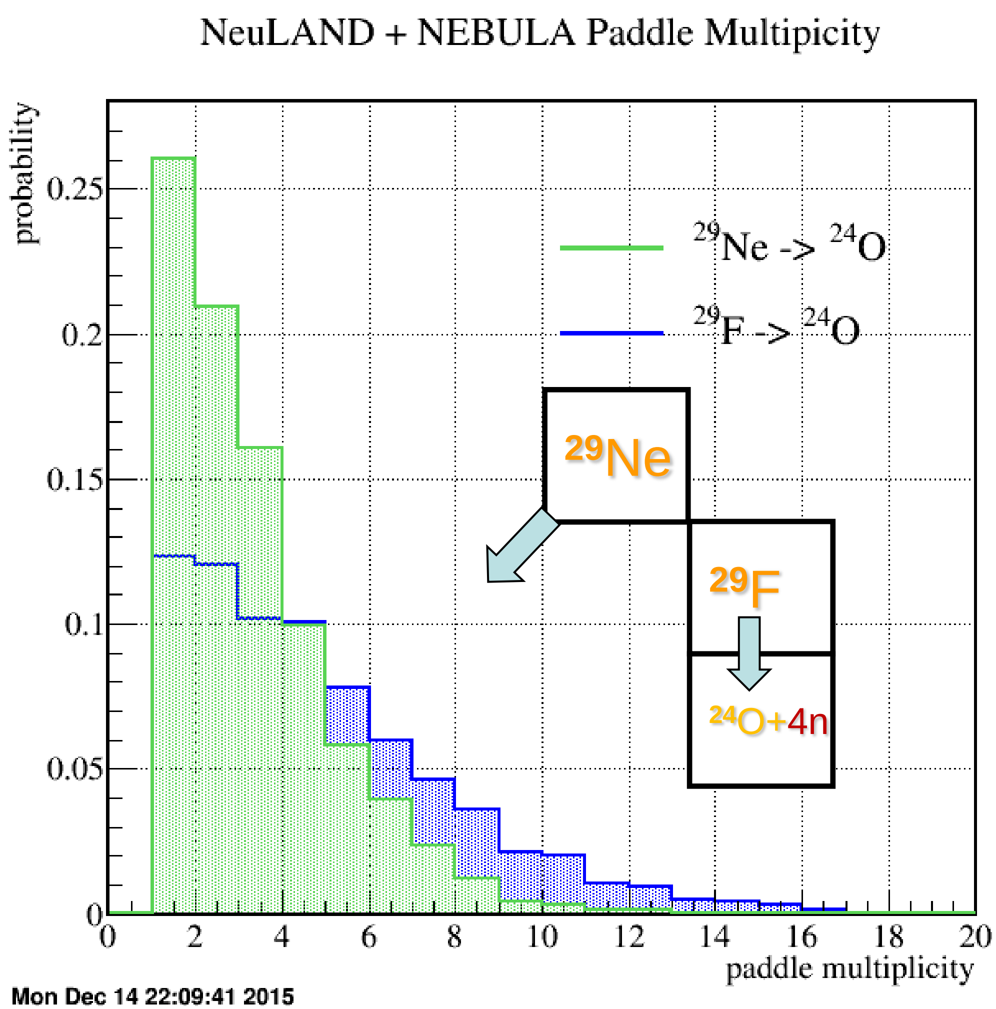

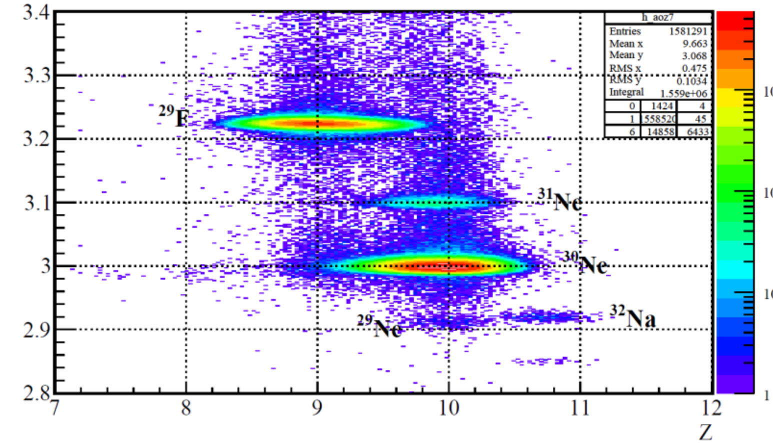

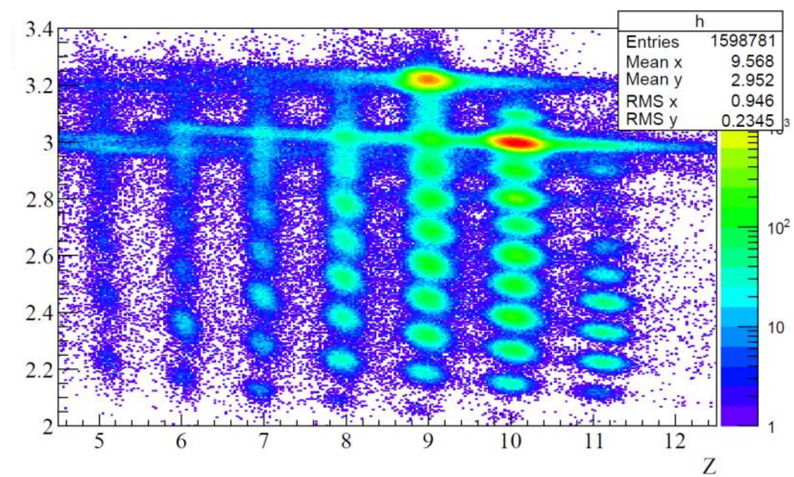

Efficiency evaluations in progress … not only ;o)

J. Kahlbow/TUDA

At the boundaries: Three body systems

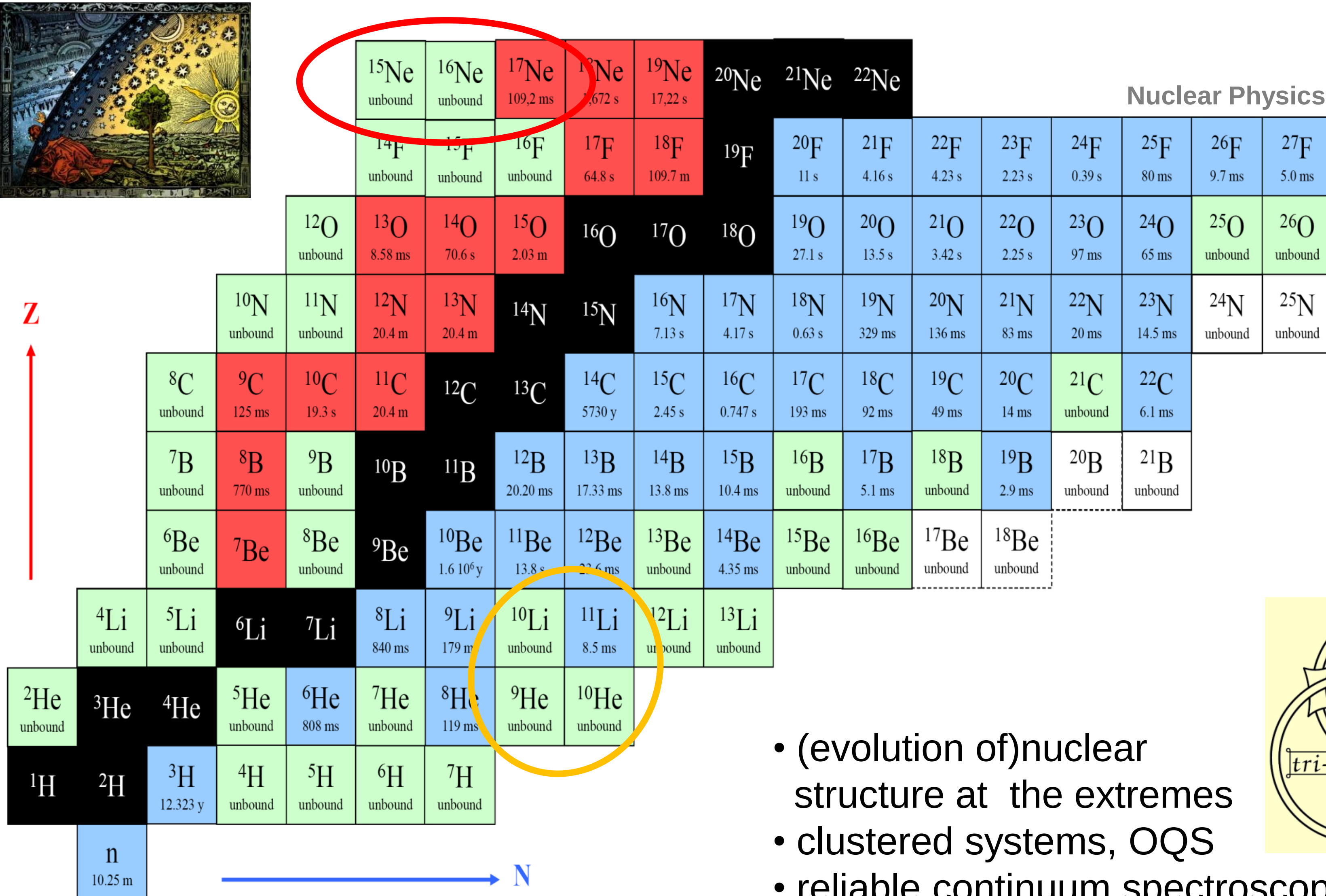

Nuclear Physics News 24 (2014) 5

- (evolution of)nuclear structure at the extremes
- clustered systems, OQS
- reliable continuum spectroscopy

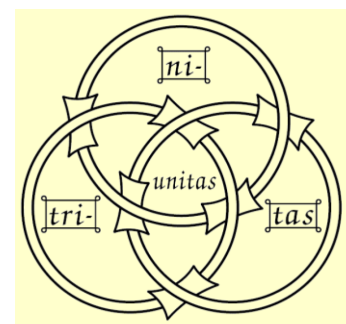

Menu

1. Breakup Experiments at high energy
   - knockout, QFS p-scattering, Coulex

2. Methods

3. Proton rich systems: $^{15\text{-}17}Ne$
   -across the proton dripline

4. Prospects/plans with new instruments

5. Summary

GSI accelerator facility …

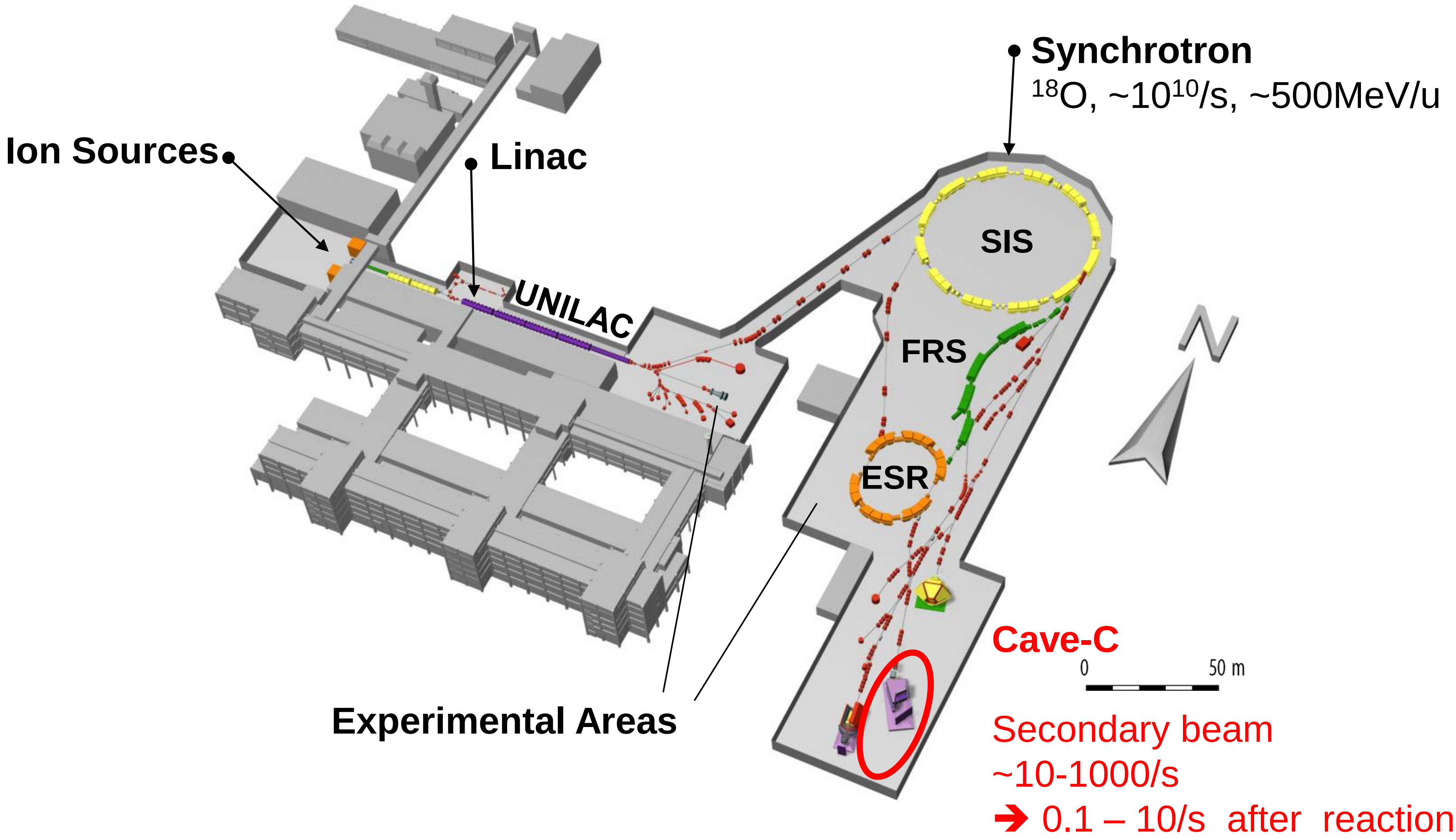

R³B/LAND Setup
(kinematically complete)

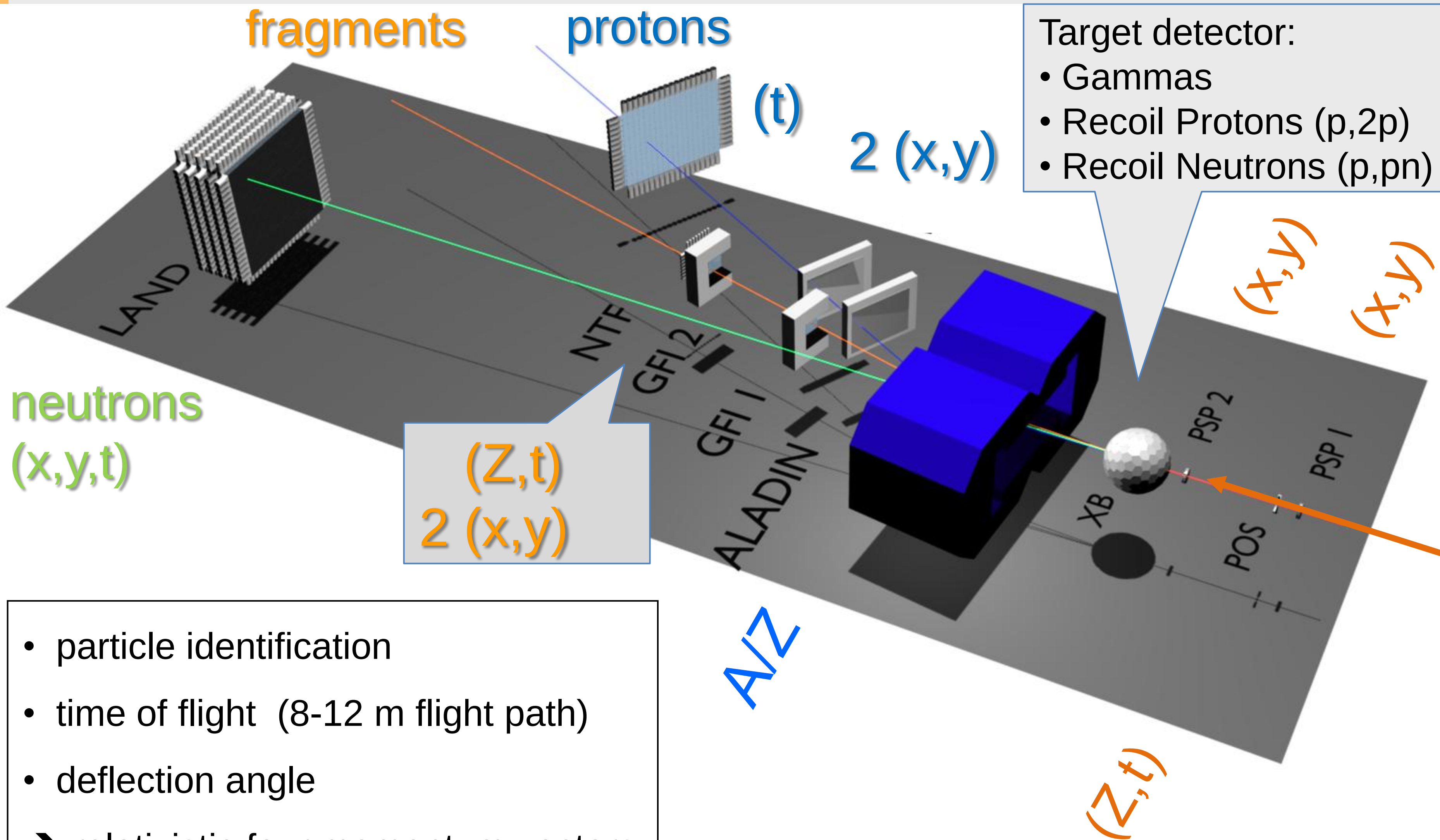

- particle identification
- time of flight (8-12 m flight path)
- deflection angle

➔ relativistic four momentum vectors

Intermediate system tells g.s. properties (n or p knockout reaction)

Observables:

Momentum knocked out neutron

missing momentum

CMS: $\mathbf{p}_m = -\mathbf{p}_{n2} = \mathbf{p}_{n1} + \mathbf{p}_f$

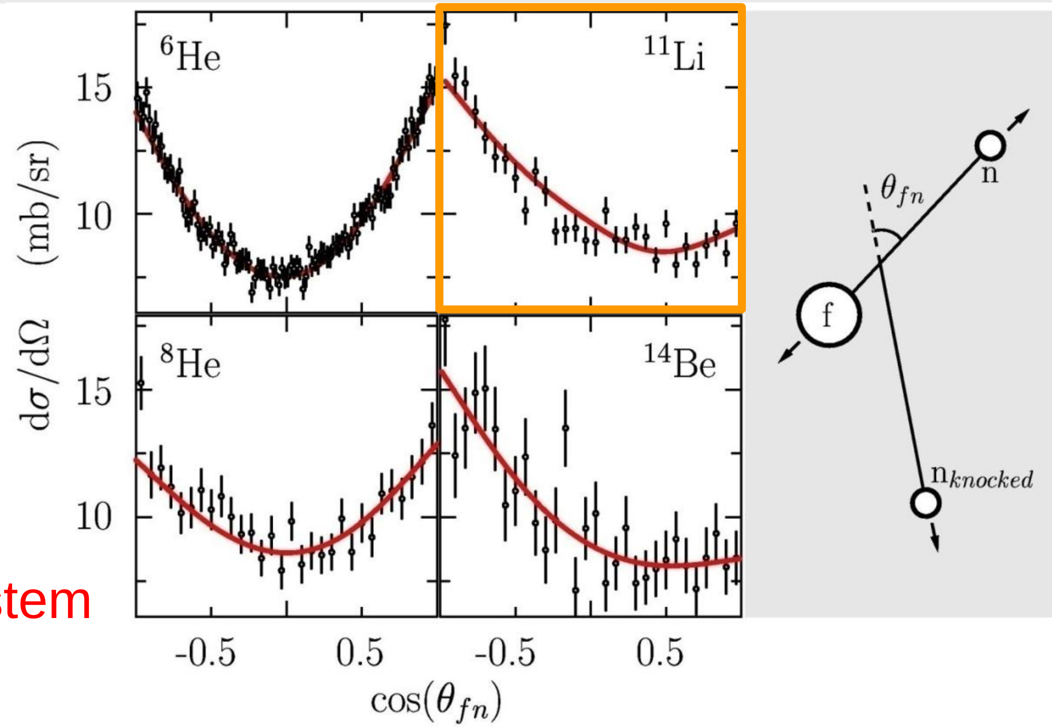

Spectroscopy of intermediate system

relative energy

CMS: $\mathbf{p}_{fn} = \mu/m_n\, \mathbf{p}_n - \mu/m_f\, \mathbf{p}_f$

Angular correlations (momenta)

$E_{fn} = p_{fn}^2 / 2\mu$

$$\cos(\theta)_{fn} = \frac{\mathbf{p}_m\, \mathbf{p}_{fn}}{p_m\, p_{fn}}$$

Sensitive observable:
Momentum profile & spectroscopy

^{10}Li | ^{11}Li

Transverse momentum
Distribution of ^{10}Li
(missing momentum)

Decomposition and position of
s and p confirmed!

similar result with energy
dependent angular correlations

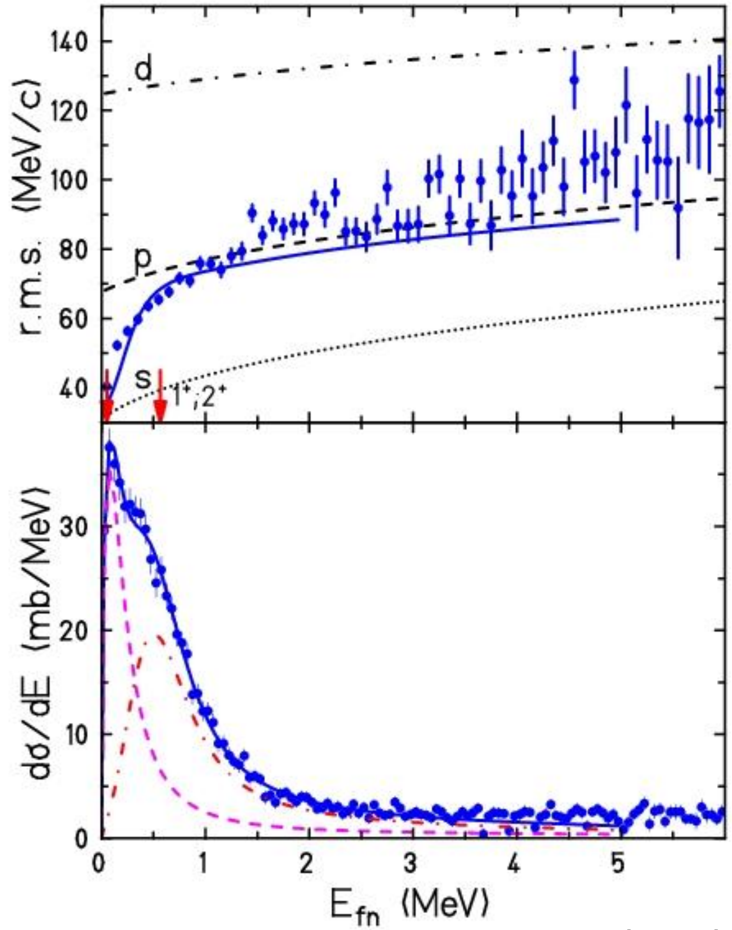

Y. Aksyutina et al.,
PLB718 (2013) 1309

2n-Model WF in ^{11}Li fit to all existing data

→ direct comparison to theory predictions

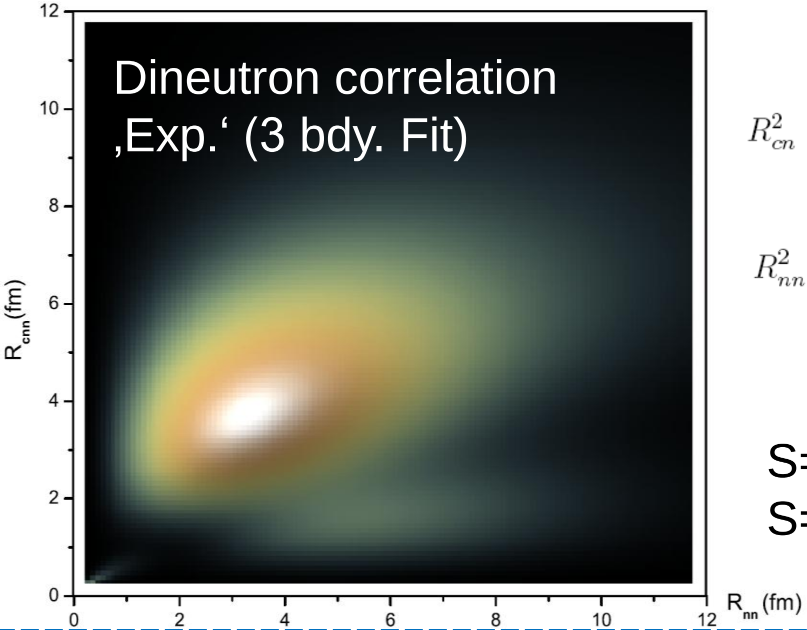

N.B. Shulgina, B. Jonson, M.V.Zhukov
Nucl. Phys. **A825**(2009)175

$$R^2_{cn} = \frac{5}{2673}\left(297 w^2_{s_{1/2},s_{1/2}}\rho^2_{s_{1/2}\,s_{1/2}} + 298 w^2_{p_{1/2},p_{1/2}}\rho^2_{p_{1/2}\,p_{1/2}} + 299 w^2_{p_{3/2},p_{3/2}}\rho^2_{p_{3/2}\,p_{3/2}} - 3\sqrt{33}\, w_{s_{1/2},s_{1/2}} w_{p_{1/2},p_{1/2}} \rho^2_{s_{1/2}\,p_{1/2}} - 3\sqrt{66}\, w_{s_{1/2},s_{1/2}} w_{p_{3/2},p_{3/2}} \rho^2_{s_{1/2}\,p_{3/2}}\right)$$

$$R^2_{nn} = \frac{1}{297}\left(297 w^2_{s_{1/2},s_{1/2}}\rho^2_{s_{1/2}\,s_{1/2}} + 298 w^2_{p_{1/2},p_{1/2}}\rho^2_{p_{1/2}\,p_{1/2}} + 299 w^2_{p_{3/2},p_{3/2}}\rho^2_{p_{3/2}\,p_{3/2}} + 30\sqrt{33}\, w_{s_{1/2},s_{1/2}} w_{p_{1/2},p_{1/2}} \rho^2_{s_{1/2}\,p_{1/2}} + 30\sqrt{66}\, w_{s_{1/2},s_{1/2}} w_{p_{3/2},p_{3/2}} \rho^2_{s_{1/2}\,p_{3/2}}\right) \quad (21)$$

S=0 (81%)
S=1 (19%)

→ $<\Theta_{12}> = 62°$

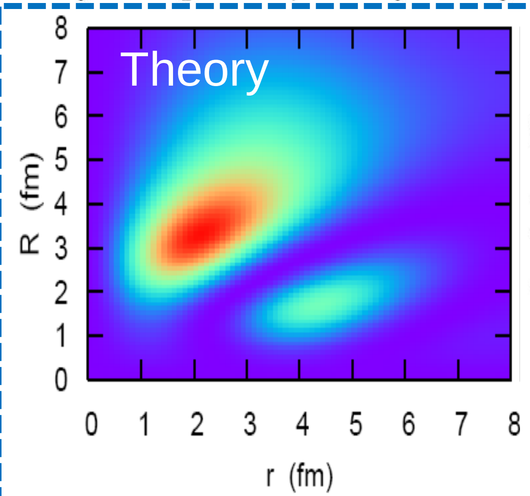

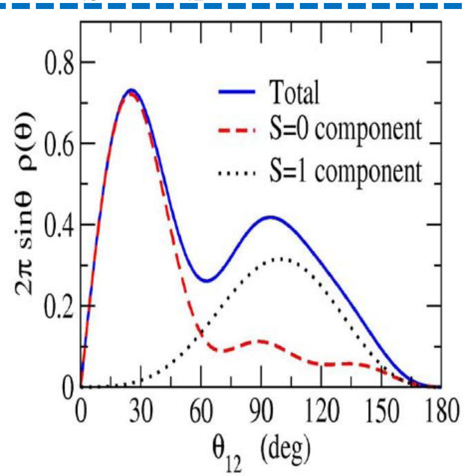

→ $<\Theta_{12}> = 66°$

K. Hagino et al., PRL 99, 022506 (2007)

$<\Theta_{12}> = 48° (+14/-18)°$

B(E1) = 1.42(18) e²fm² (< 3MeV)
cluster sum-rule, matter radius
T. Nakamura et al.

^{17}Ne a potential 2p halo

"^{17}Ne is a proton-dripline nucleus,
with strong indications of having a 2p – halo"

*Zhukov & Thompson, PR**C** 52 (1995) 3505*

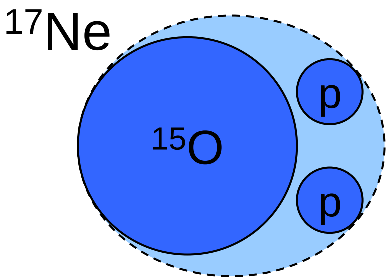

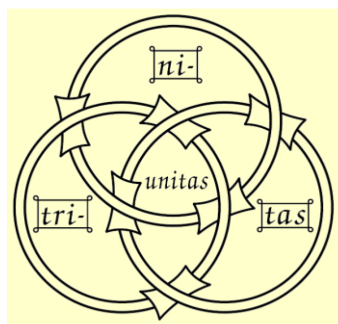

- S_{2p} = 943 keV, S_p = 1479 keV
- $T_{1/2}$ = 109.2 ms (β^+ to ^{17}F)
- Groundstate J^π=1/2$^-$; no bound exc. states

*W. Geithner, T.Neff et al, PRL **101** 252502 (2008)*

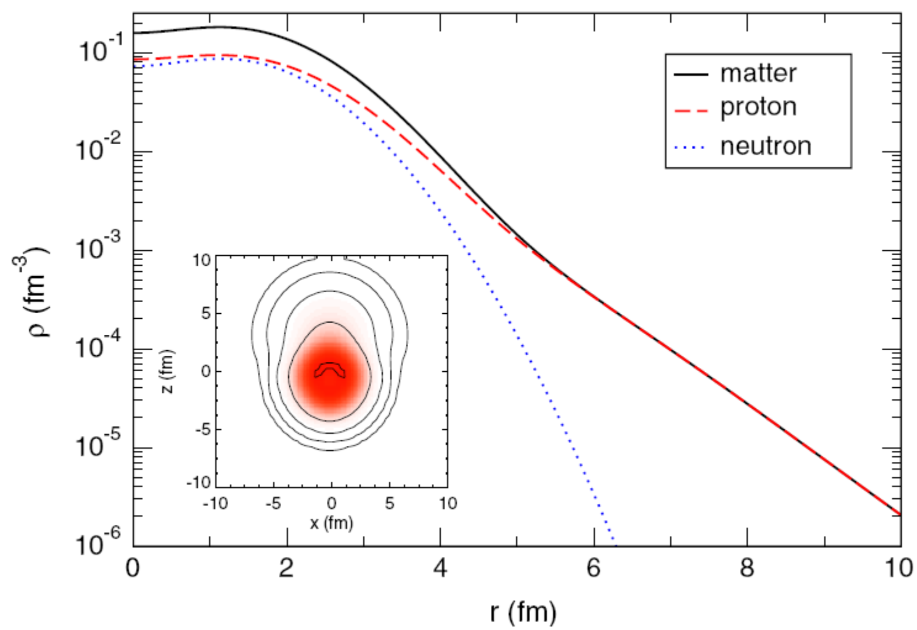

Looking for halo signatures

Large fraction of the valence protons in the classically forbidden region ?

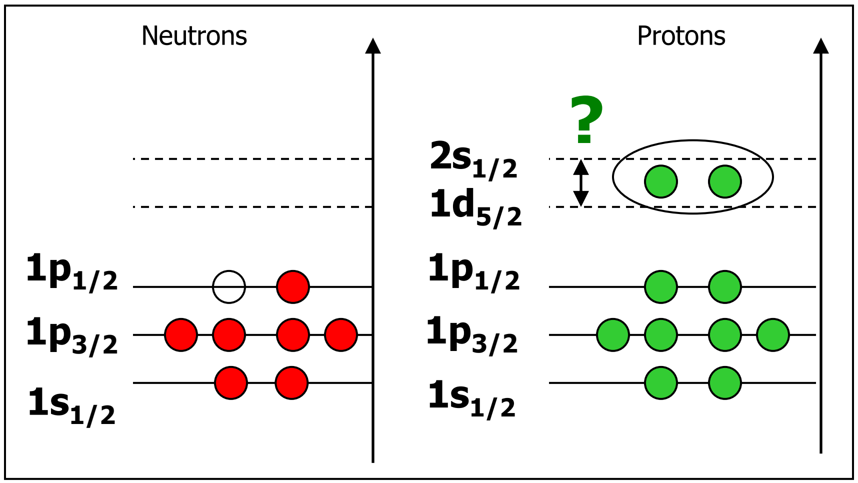

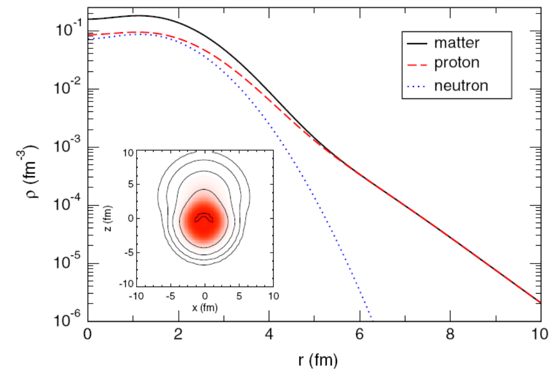

*W. Geithner, T.Neff et al, PRL **101** 252502 (2008)*

Coulomb wall in addition
to angular momentum barrier (s,d)…
➔ search for strong s^2 configuration

- *Grigorenko et al., PRC 71 (2005) 051604(R).*
  - 3-body cluster model: s^2 content 48%.
- *Geithner&Neff et al., PRL 101 (2008) 252502.*
  - Charge radius measurement + FMD: 42% s^2.
- *Tanaka et al., PRC 82 (2010) 044309.*
  - Reaction cross-sections: Long tail in ^{17}Ne matter density, dominant s^2 configuration.
- *Oishi et al., PRC 82 (2010) 024315.*
  - 3-body model: s^2 content 15%.

One-proton knockout from ^{17}Ne – ^{16}F relative energy Spectrum

F. Wamers

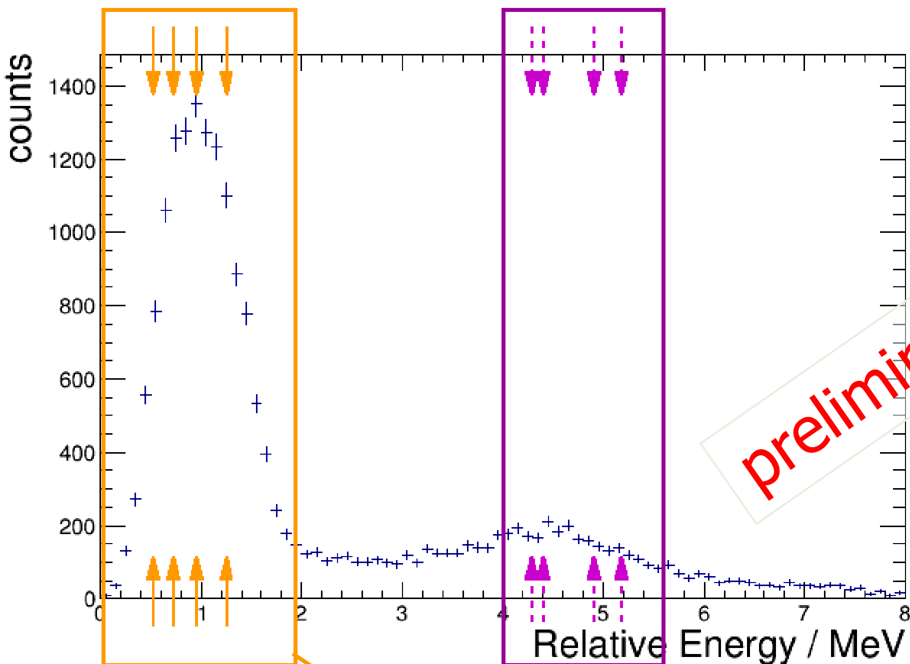

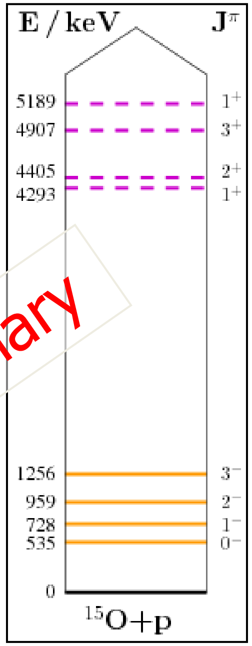

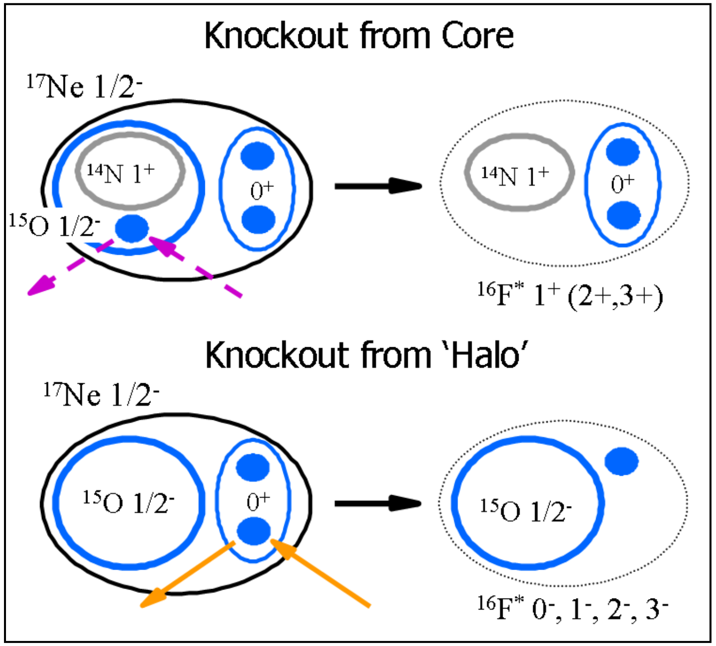

Grigorenko, PRC 71 (2005) 051604(R).

Exclusive selection of knockout from valence protons

$$\vec{p}_{proton} = -\vec{p}\left({}^{16}F\right)$$

Halo-Proton Knockout from ^{17}Ne: ^{16}F (=^{15}O+p) Transverse Momentum Distribution

F. Wamers

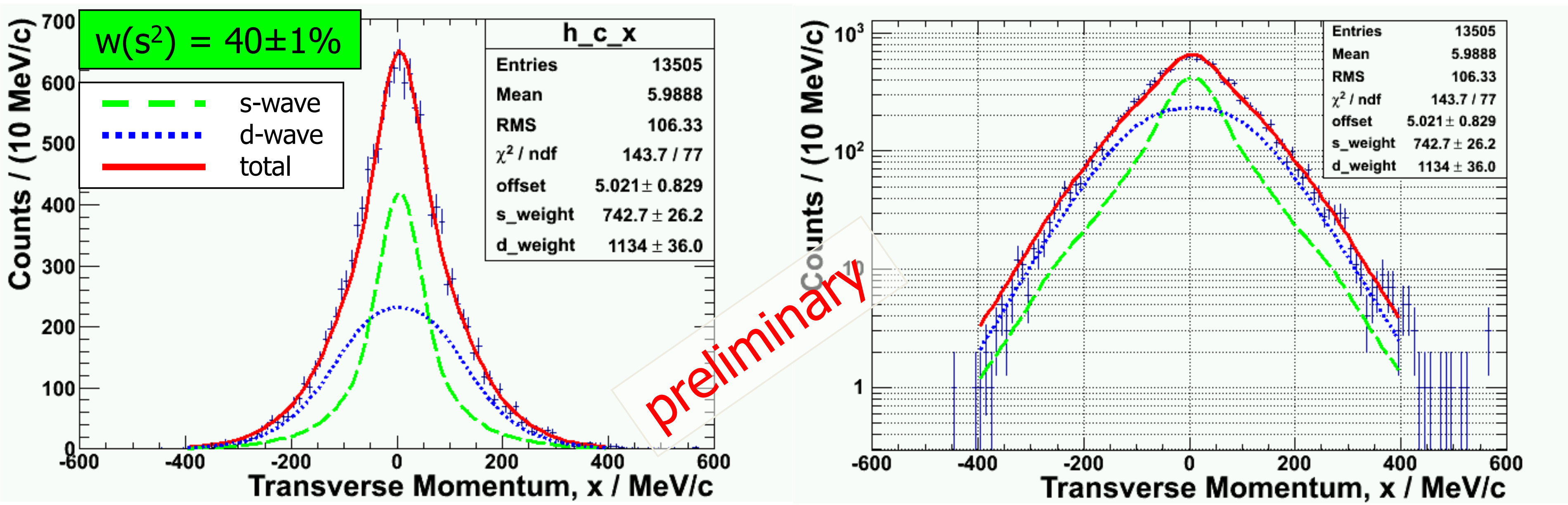

Glauber-type calculation (MOMDIS): 1s/0d single-particle p-removal from ^{16}F+p
Bertulani et al., CPC 175 (2006) 372

- s-wave c ont ents ~40% in the ^{17}Ne halo (p$_x$: 39.6±1.1 %, p$_y$: 40.4±1.1 %)
- Moderate halo character of ^{17}Ne confirmed
- Good agreement with Grigorenko et al., and with Geithner/Neff et al.

Momentum Profile (^{16}F)

F. Wamers

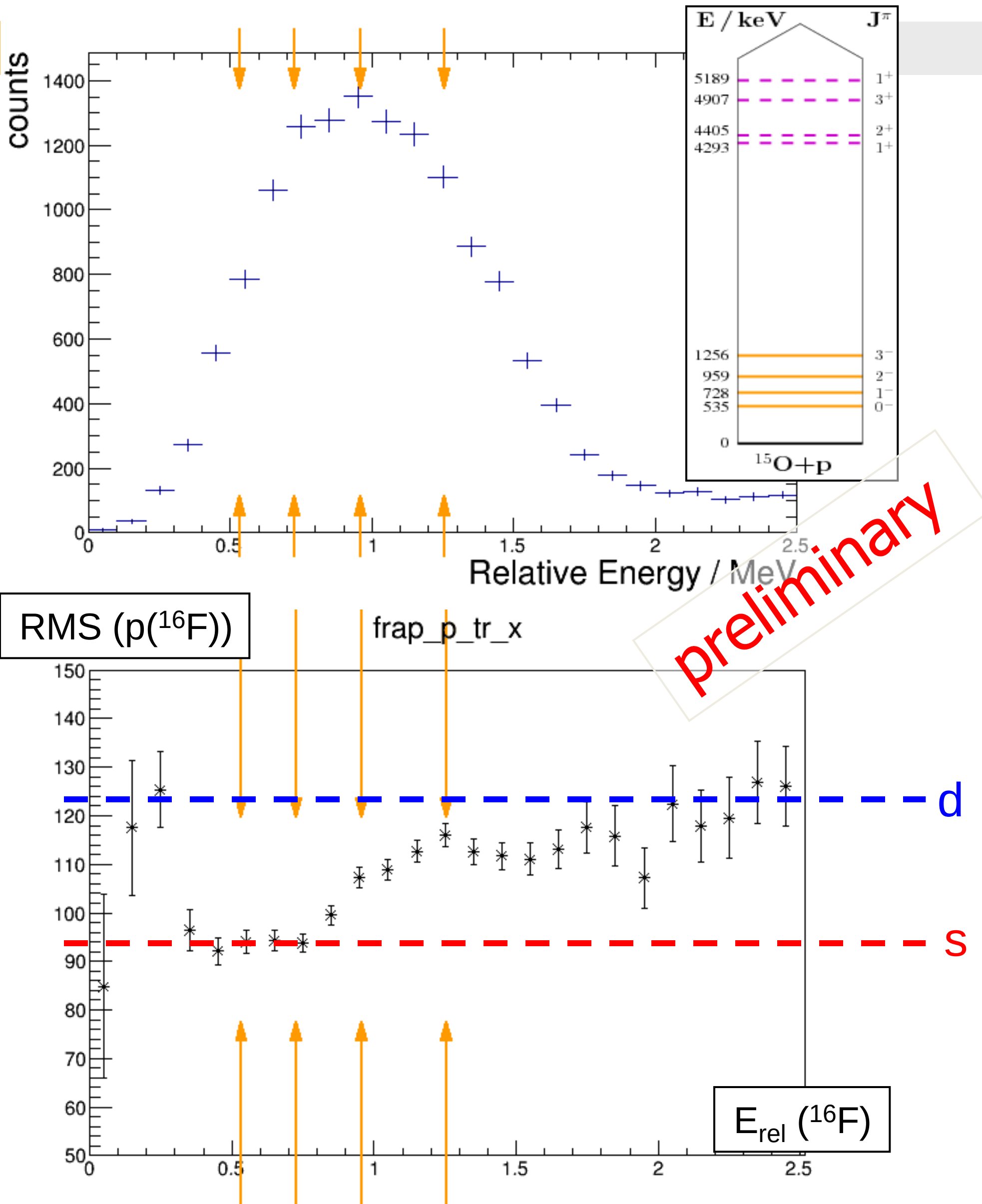

Eikonal Theory (MOMDIS)

RMS (s):	92.3 MeV/c
RMS (d):	123.1 MeV/c

^{16}F momentum profile around1 MeV: consistent with calculation for knocked out valence p's.

- Step-like increase, s- to d-protons (^{16}F negative-parity states)

(C. Bertulani, MOMDIS)

Momentum Profile (^{16}F)
a different view

MOMDIS calculation for Rrel dependent width

RMS (E)=

w_s (E) * RMS $_s^{theo}$ (E) +
w_d (E) * RMS $_d^{theo}$ (E)

w_s, w_d from fit to relative energy spectrum for the respective energy bins.

➔ Consistent description in peak region
➔ Ambiguities for high and low part of energyspectrum (e.g. in the presence of non-resonant bg. !
➔ Clear Advantages using momentum profile method

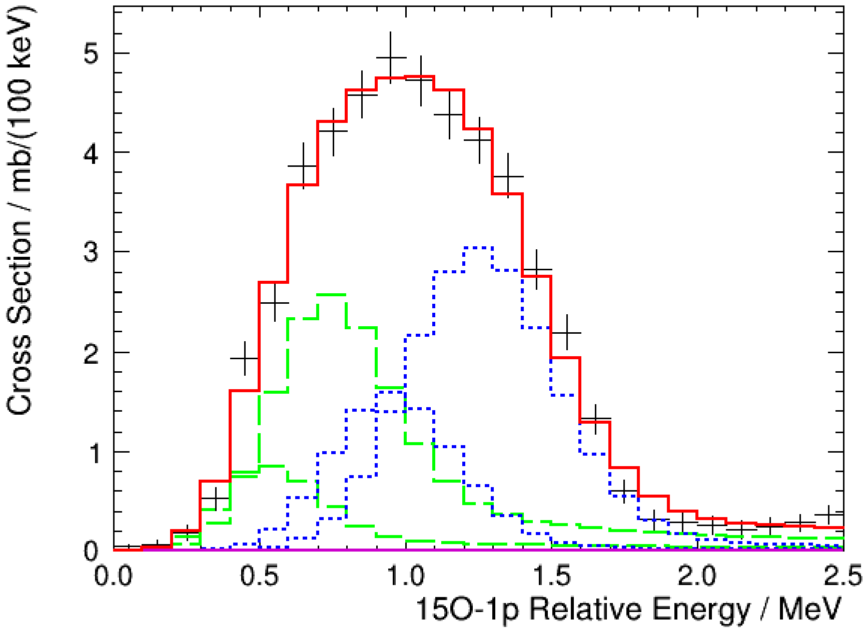

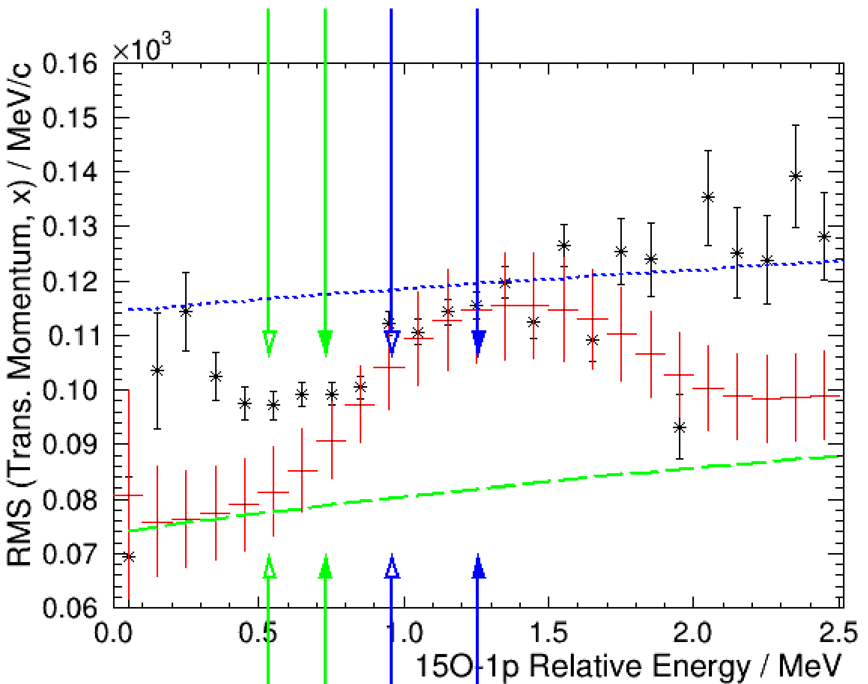

Crossing the Proton Dripline to ^{15}Ne

F. Wamers

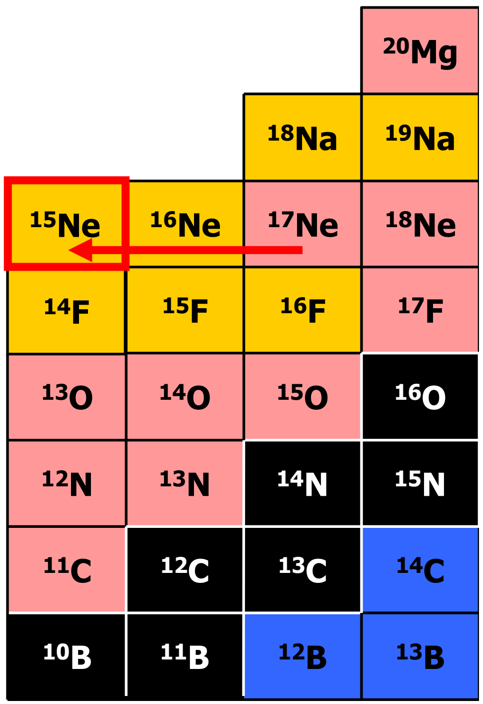

Two-neutron Knockout

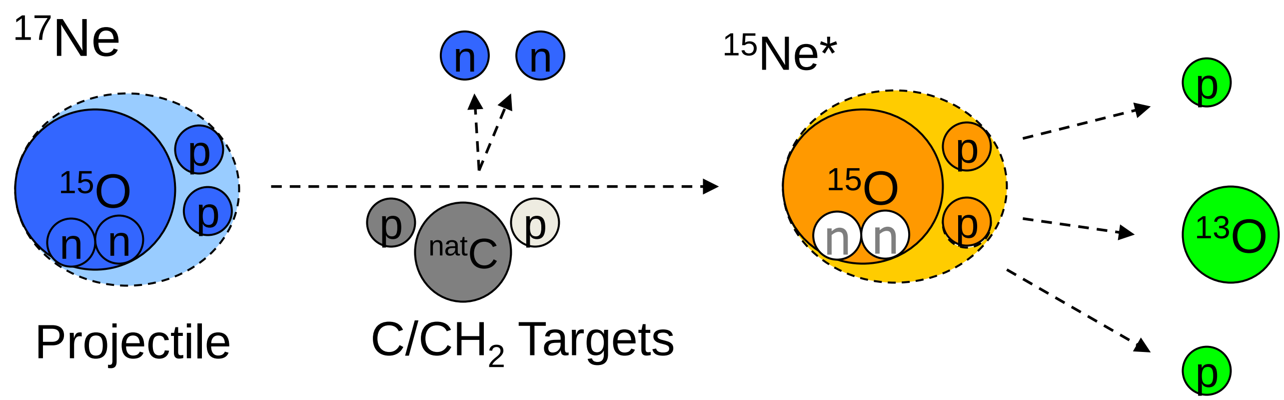

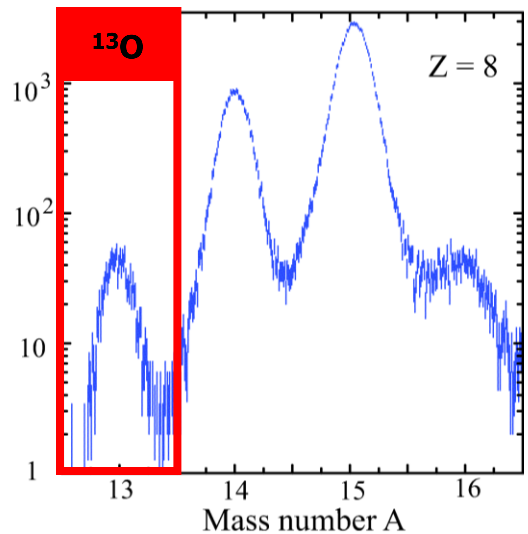

^{13}O + 2 proton FSI

→ ^{15}Ne 3-body relative-energy spectrum

→ 3-body angular correlations

First Observation and spectroscopy of ^{15}Ne

F. Wamers et al., PRL 112, 132502 (2014)

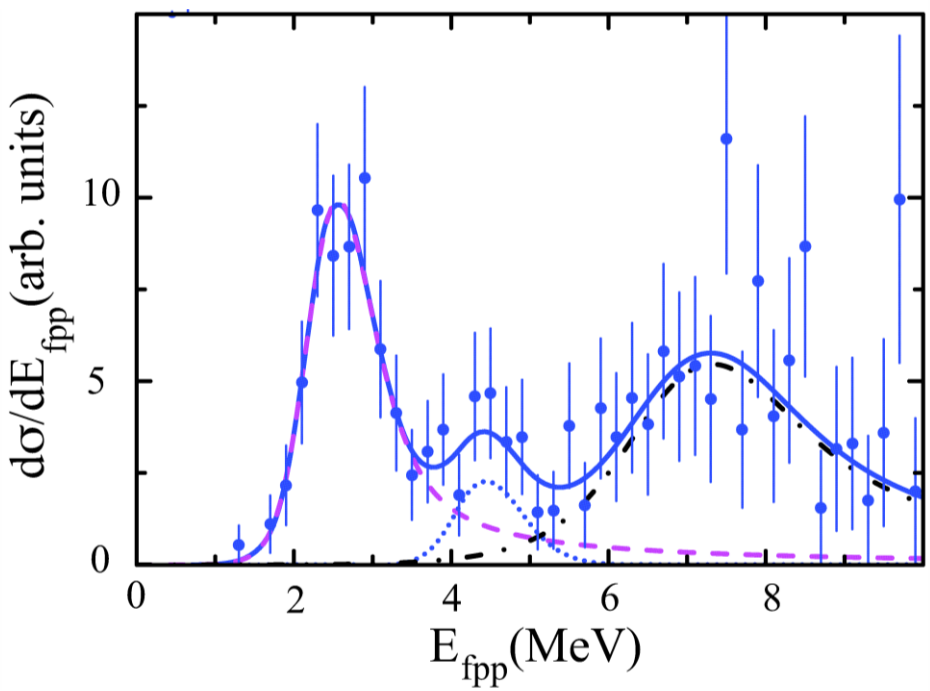

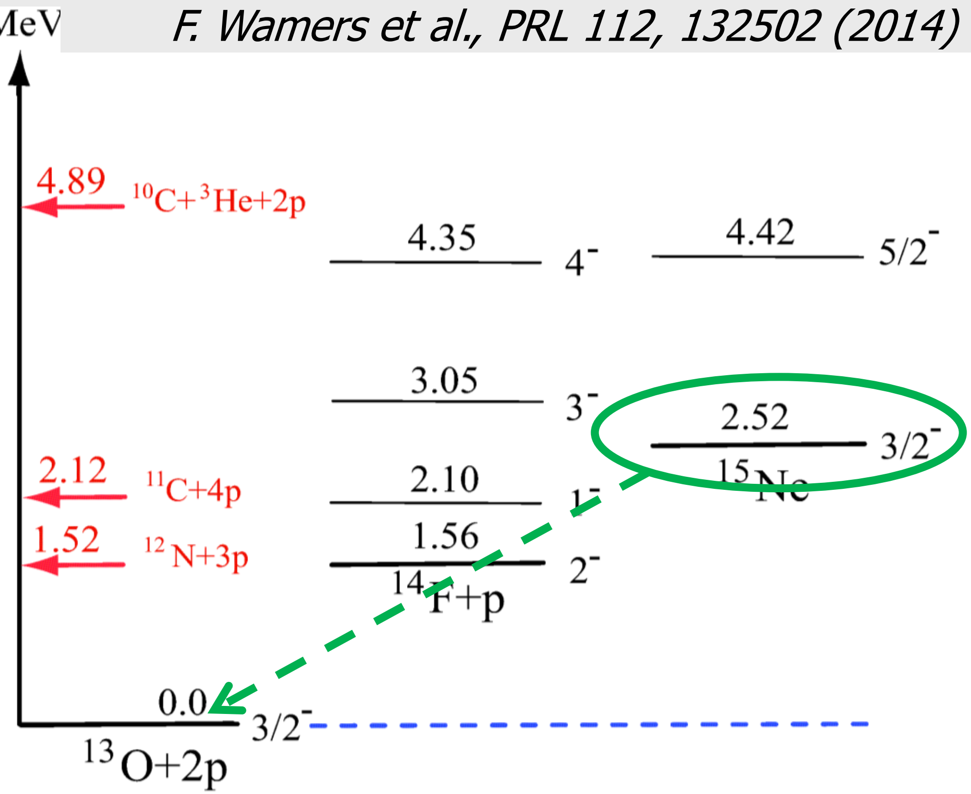

- Groundstate
Er = 2.522(66), Γ = 0.59(23) MeV
- 1st exc. State
Er = 4.42(4), Γ ≤ 0.1 MeV
- (2nd) exc. States
Er around 7-9, Γ around 2.5 MeV

- ^{15}Ne ground state unbound
  S_{2p} = 2.522(66) MeV
- Corresponds to mass excess
  ME(^{15}Ne) = 40.215(69) MeV
- Good agreement with *model prediction*:
  S_{2p} = 2.68(24) MeV

H.T. Fortune, Phys. Lett. B 718, 1342 (2013)

Description of the three body continuum

- Reduction (CMS, E*, rot. inv)

  9 variables $\rightarrow$ 2 variables **(ε, θ)**

ε is the fractional energy for a subsystem (e.g. $\varepsilon = E_{nn}/E_{nnf}$)

θ is the angle between the relative momenta (e.g. p_{nn}, $p_{f\text{-}nn}$)

- Three body correlation function (expansion in hyperspherical harm.):

$$W(\varepsilon,\theta) \propto \frac{d^2\sigma}{d\varepsilon d\theta} \propto \sum_{\alpha,\alpha'} C^{\dagger}_{\alpha'} C_{\alpha} \mathcal{Y}^{\dagger}_{\alpha'}(\varepsilon,\theta)\mathcal{Y}_{\alpha}(\varepsilon,\theta)$$

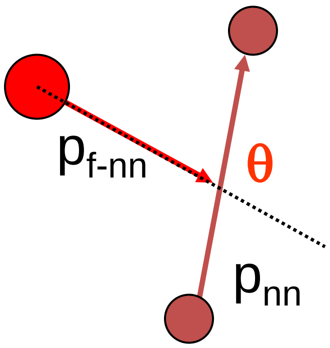

- Complex coefficients C depend on quantum numbers $\alpha = \{K, L, S, l_x, l_y\}$

L.V. Chulkov, H.S., I.Thompson, et al., NPA759 (2005) 23

M.Meister, L.V. Chulkov, H.S., et al., PRL91 (2003) 16504

Characterization of the decays

F. Wamers et al., PRL 112, 132502 (2014)

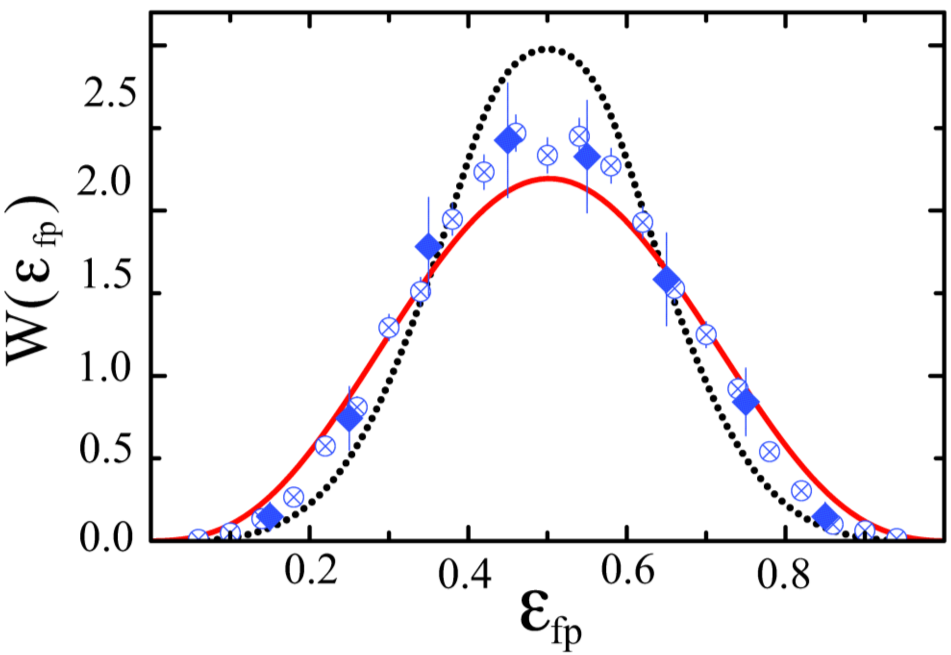

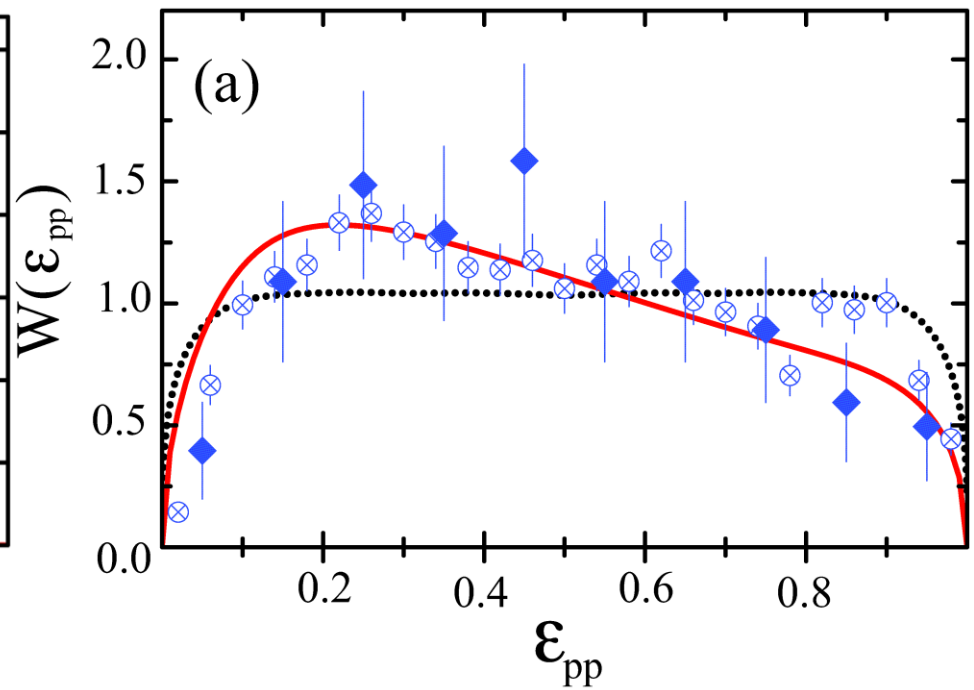

⊗ ^{16}Ne exp data

♦ ^{15}Ne exp data

Calculation of ^{16}Ne isotropic 3-body decay

Calculation of ^{15}Ne sequential decay via the ^{14}F ground state

L.V. Grigorenko, I.G. Mukha, I.J. Thompson, and M.V. Zhukov, Phys. Rev. Lett. 88, 042502 (2002).

^{15}Ne decay shows a genuine 3-body character, despite intermediate states in ^{14}F.

EPJ A Highlight - Mechanisms of two-proton emission seen in three-body correlations

J. Marganiec et al., EPJ A (2015) 51: 9

Published on Tuesday, 10 February 2015 16:14

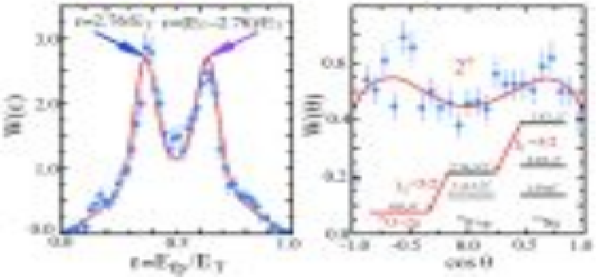

Sequential two-proton decay of the ^{16}Ne E_r=7.57 MeV state. The fractional energy distribution (left) gives resonance energy in ^{15}F while the angular distribution (right) determines I^{π} of the initial state.

Hitherto three-body correlations between decay products of nuclear resonances, unstable to the emission of two neutrons have been a very effective tool in the analysis of GSI-experiments on ^{5}H, ^{10}He, ^{13}Li, and ^{14}Be. Here the first report is given about the mechanisms for two-proton emission from states in ^{16}Ne, representing the presently most complete study of this nucleus. One-neutron knockout from ^{17}Ne populated the ^{16}Ne(g.s.) (E_r=1.39 MeV, Γ=0.08 MeV) above the ^{14}O+p+p threshold, and resonances at E_r=3.22 MeV and 7.57 MeV. The decay mechanisms were revealed analysing three-body energy correlations in the ^{14}O+p+p system. It was found that the ^{16}Ne(g.s.) undergoes a democratic three-body decay. In contrast to this, the ^{16}Ne(21+) state emits protons through the ^{15}F(g.s.) sequentially. The decay of 7.57 MeV state is well-described assuming emission of a proton from the $d_{5/2}$ shell to ^{15}F($5/2^+$), which decays by $d_{5/2}$ proton emission to ^{14}O(g.s.). By using R-matrix analysis and mirror symmetry this state was unambiguously identified as the third 2^+ state in ^{16}Ne.

^{16}Ne relative energy spectrum

F. Wamers et al., PRL 112, 132502 (2014)

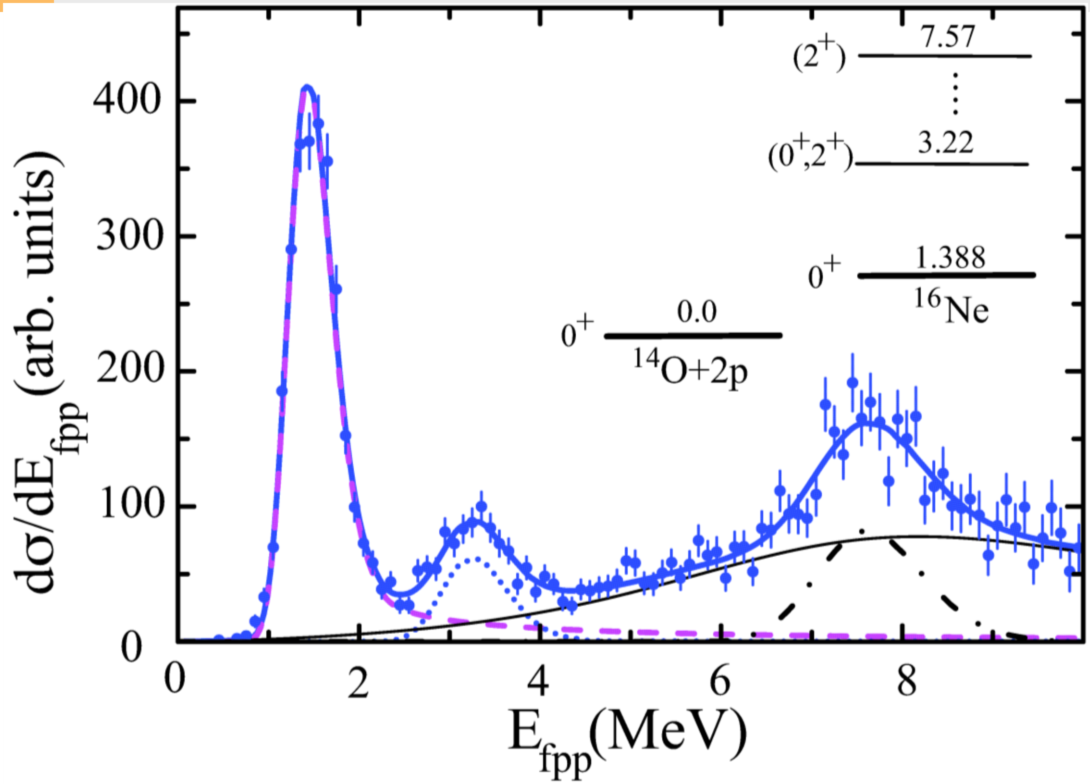

$I^\pi = 0^+$		$I^\pi = (0^+,2^+)$		$I^\pi = (2^+)$		
E_r	Γ	E_r	Γ	E_r	Γ	Ref.
1.388(15)	0.082(15)	3.22(5)	≤ 0.05	7.57(6)	≤ 0.1	[⋆]
1.33(8)	0.2(1)	3.02(11)	–	–	–	[11]
1.466(45)	–	–	–	–	–	[12]
1.399(24)	0.11(4)	–	–	–	–	[13]
–	–	3.5(2)	–	–	–	[14]
1.35(8)	–	–	–	7.6(2)	$0.8(^{+4}_{-8})$	[15]

[11] G.J. KeKelis et al., Phys. Rev. C 17, 1929 (1978).
[12] G.R. Burleson et al., Phys. Rev. C 22, 1180 (1980).
[13] C.J. Woodward, R.E. Tribble and D.M. Tanner, Phys. Rev. C 27, 27 (1983).
[14] K. Föhl et al., Phys. Rev. Lett. 79, 3849 (1997).
[15] I. Mukha et al., Phys. Rev. C 79, 061301(R) (2009)

Confirmation of previous results.
Narrow width for
1st and 2nd excited state.

K.W. Brown et al,
Phys.Rev.Lett. 113, 232501 (2014)
gs. Er=1.476(20) Γ<80keV
„width puzzle“

The quest for the ^{17}Ne Halo – Coulomb dissociation

J. Marganiec

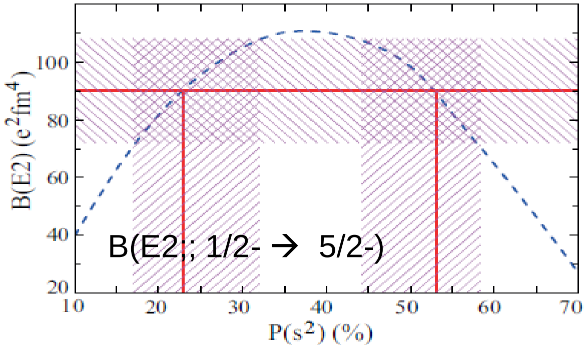

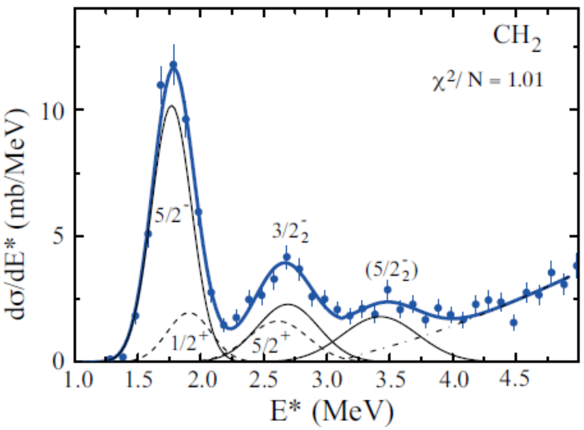

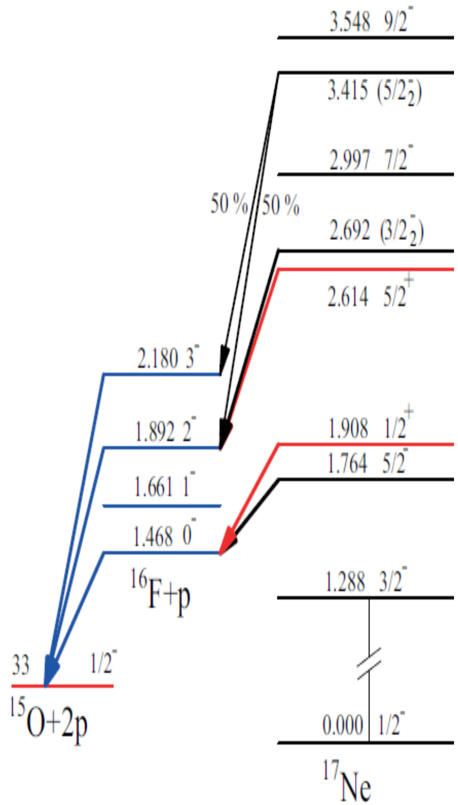

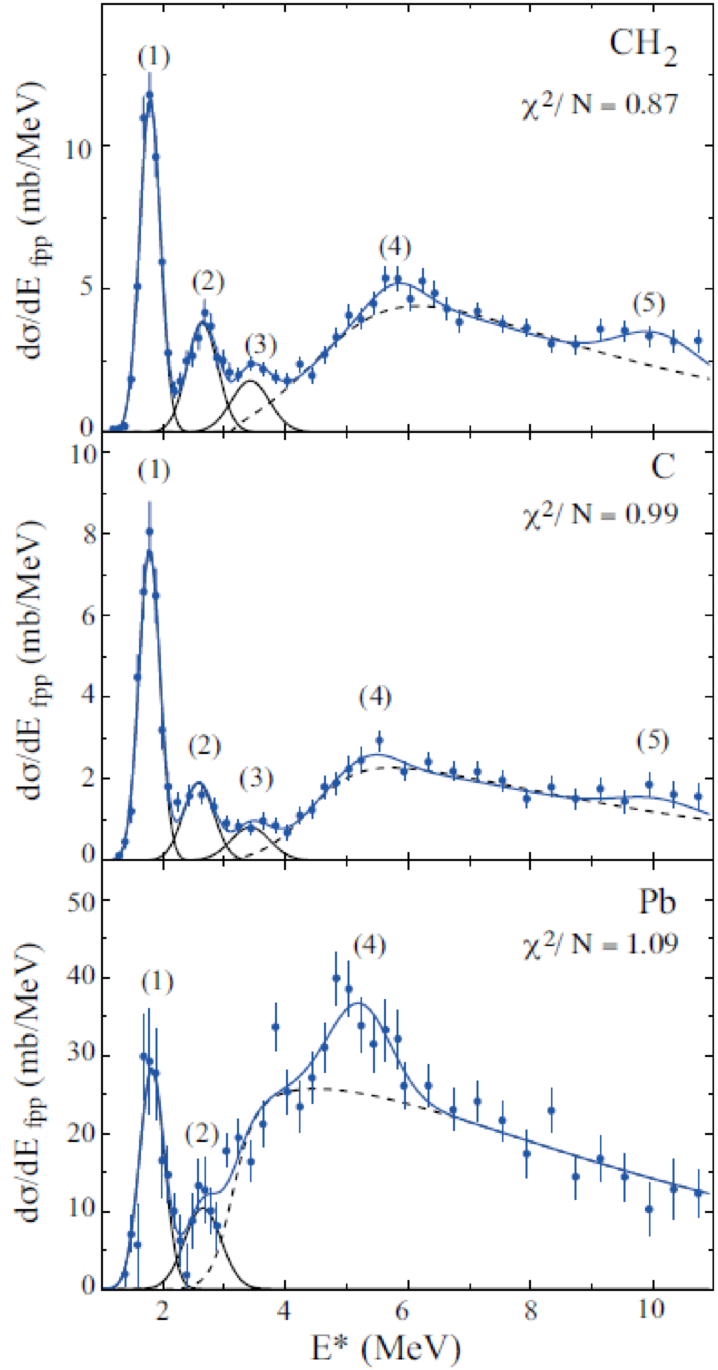

V. Guimarães et. al, Phys. Rev. C **58**, 116 (1998).

H.T. Fortune *et al.*, Phys. Rev. C **20**, 1228 (1979).

The quest for the ^{17}Ne Halo
– Looking for soft dipole modes …

J. Marganiec

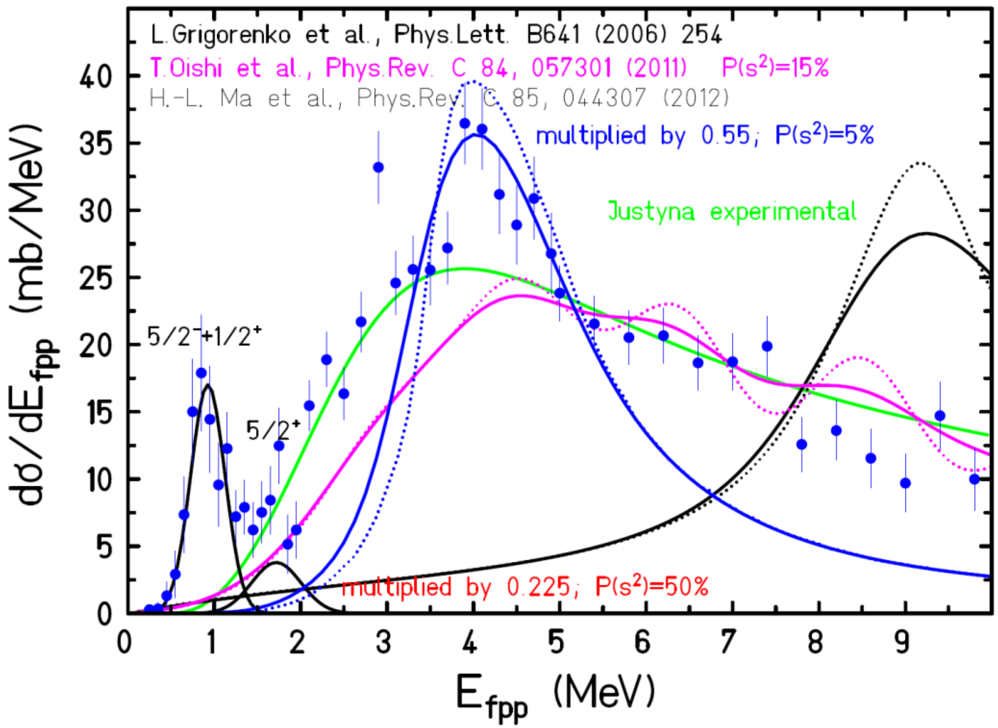

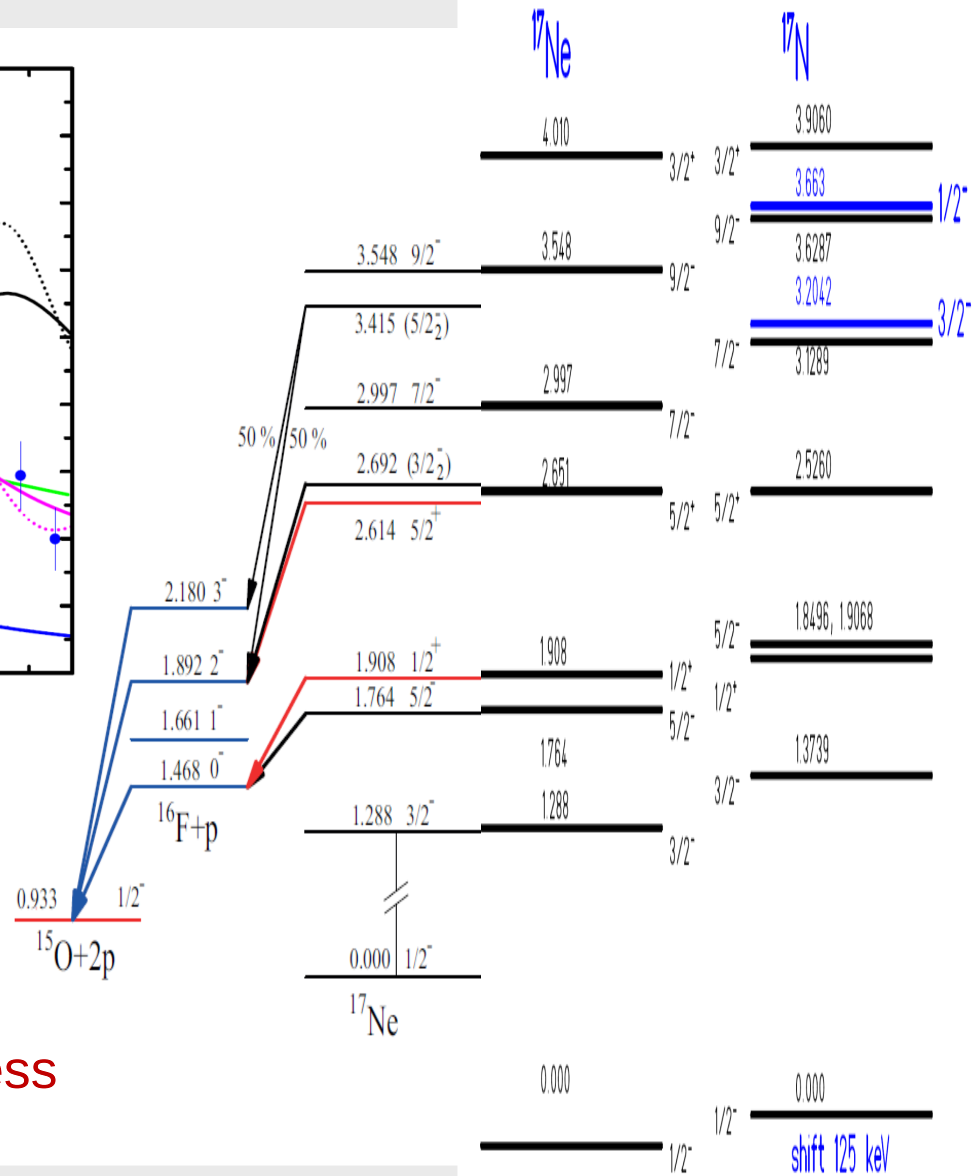

Not yet conclusive, work in progress

Summary / Outlook

- Nuclear systems at the extremes cleanly produced and analyzed
- Largest neutron/proton asymmetries
- Rôle of seed nuclei discussed, correlations analyzed
- Frontier line: Oxygen isotopes

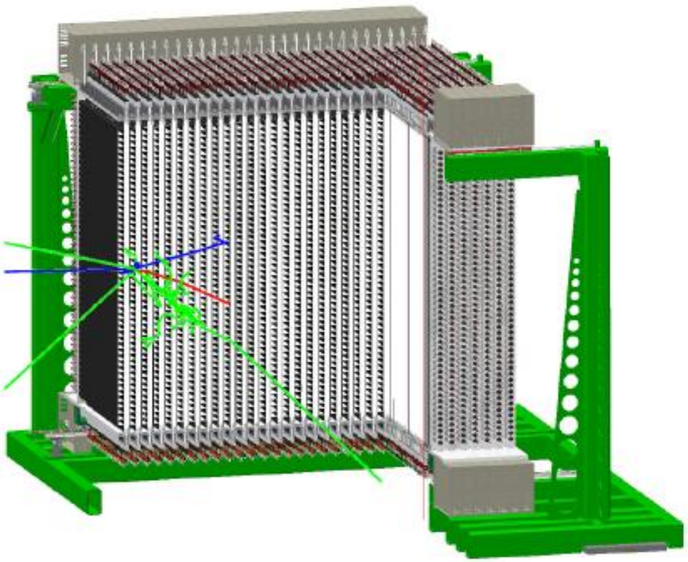

- New Detectors ➔ better sensitivity
- New facilities ➔ higher intensity

➔ f + n + n + n + n (e.g. ^{7}H) in reach

7H ↓ and 4n →

4He(8He; 8B) @ 186 MeV/u

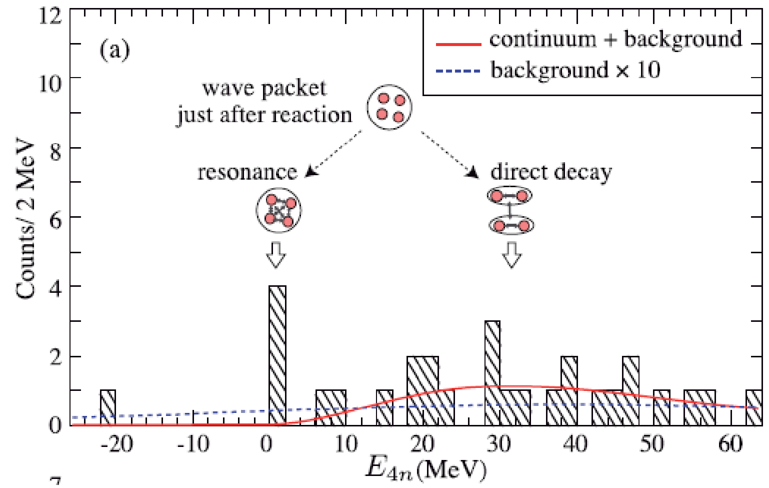

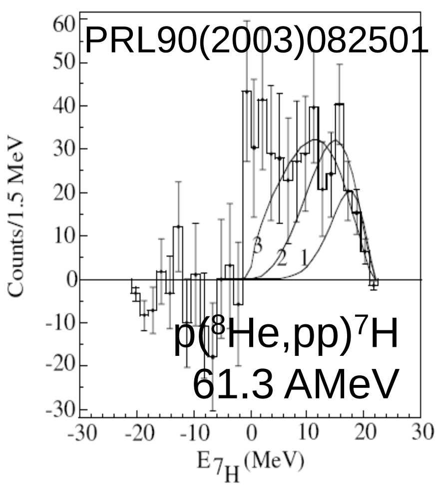

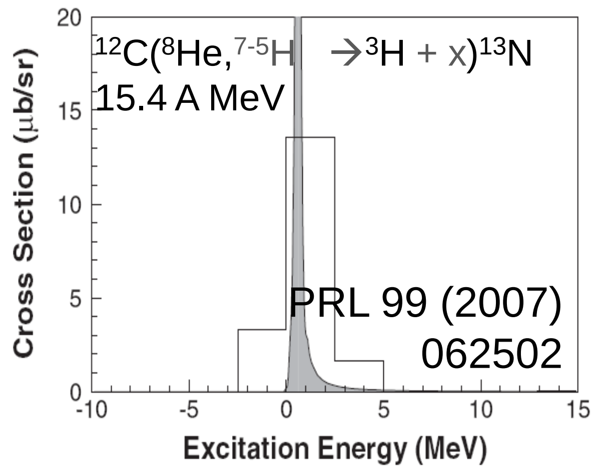

- Improvement by exclusive measurements

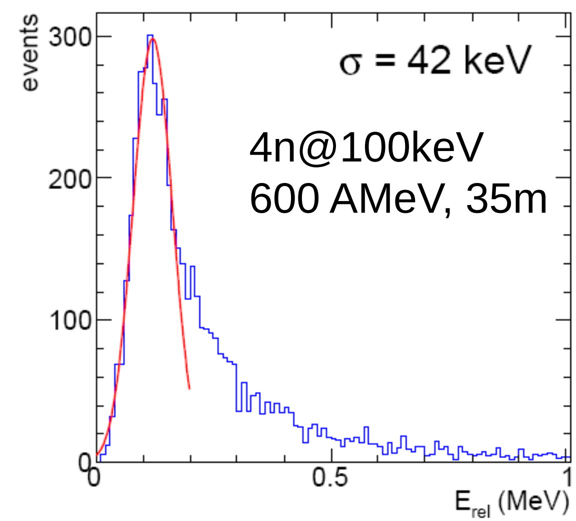

NeuLAND Simul.

EPJA 32 (2007) 261

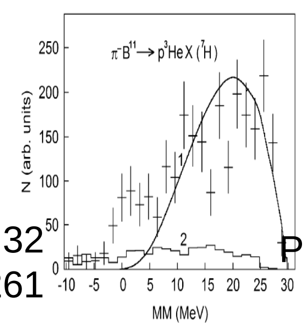

PRC81 (2010) 064606

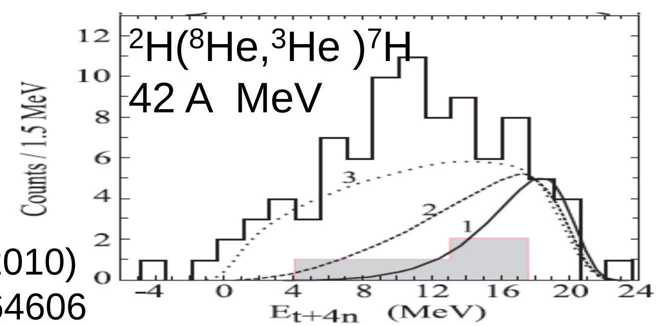

GLAD @ Cave-C

Short Spec.:
Bℓ = 4.8 Tm
Opening angle: 80 mrad
20 mT field @ target position

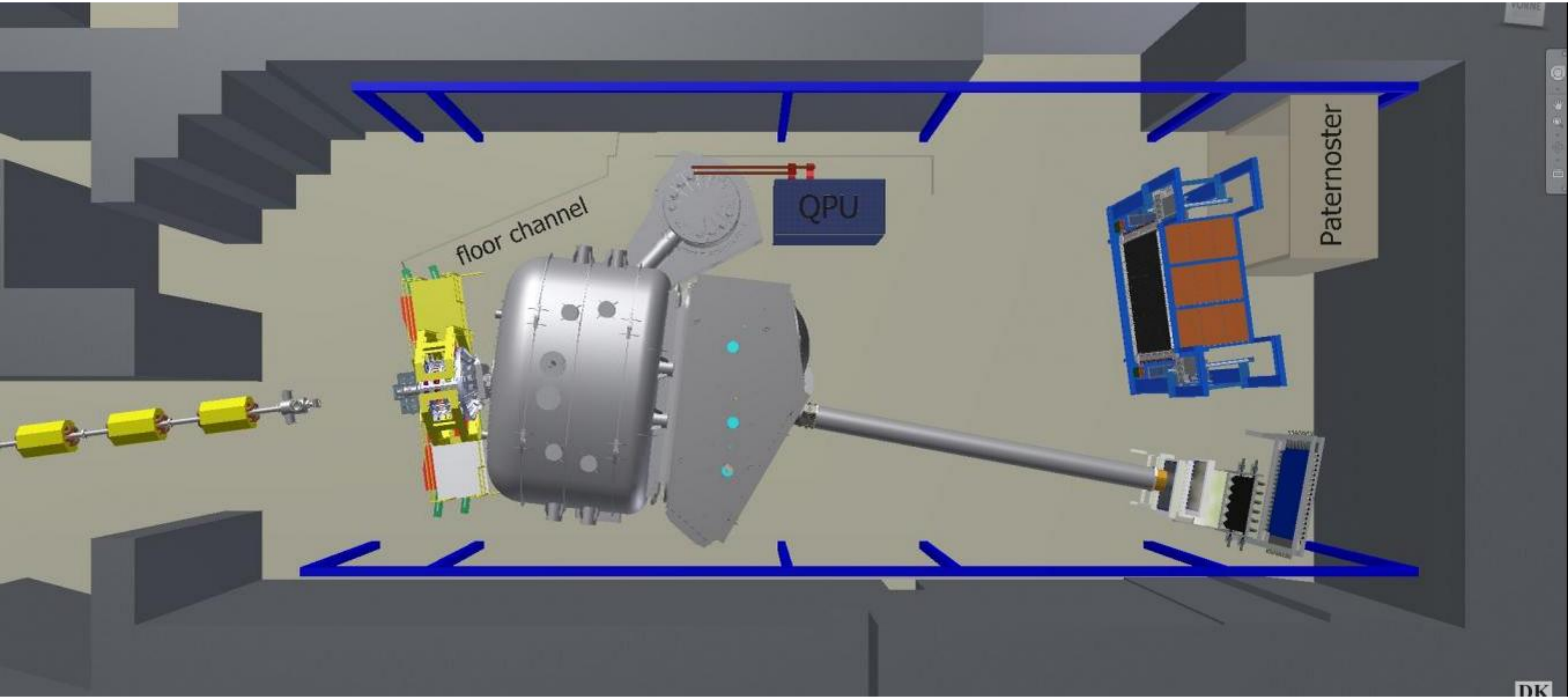

Schedule and first experiments

2014	Installation of 20% detectors NeuLAND and CALIFA Commissioning run in Q3/2014
2015/16	Construction and installation of detector components
2017/18	Commissioning of full R3B setup (Cave C)
2018-202x	Physics runs at GSI (Cave C) (phase 0)
202x-202x+1	Move to High-Energy Branch building
202x+1 →	Commissioning and first experiments at Super-FRS (phase 1)

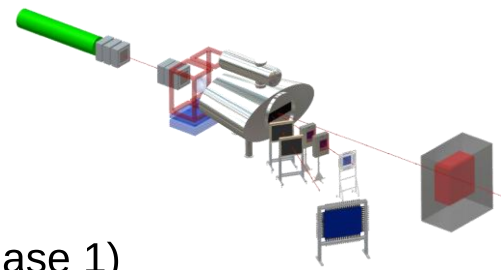

Experiments will make use of uniqueness of R^{3}B:

- Reactions at high beam energies up to 1 GeV/nucleon
- Tracking and identification capability even for the heaviest ions
- Multi-neutron tracking capability, high-efficiency calorimeter

Experiments possible for the first time:

- 4 neutron decays beyond the drip-line and for heavier n-rich isotopes
- Kinematically complete measurements of quasi-free nucleon knockout reactions
- Electric dipole and quadrupole response of Sn nuclei beyond N=82, and of neutron-rich Pb isotopes (polarizability, symmetry energy)
- fission barriers from (p,2p) reactions (→ r-process)

Dipole strength Distributions in heavy neutron-rich nuclei

- core vs. neutron skins & halos → density / asymmetry

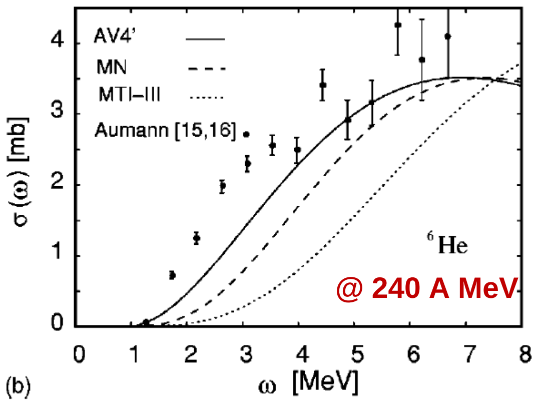

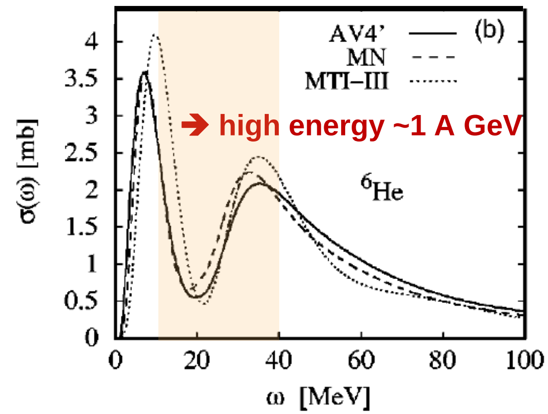

S. Bacca et al.
PRL **89** (2002) 052502
PRC **69** (2004) 057001

- access to EoS (e.g. neutron star) & low lying E1 strength (r-process)

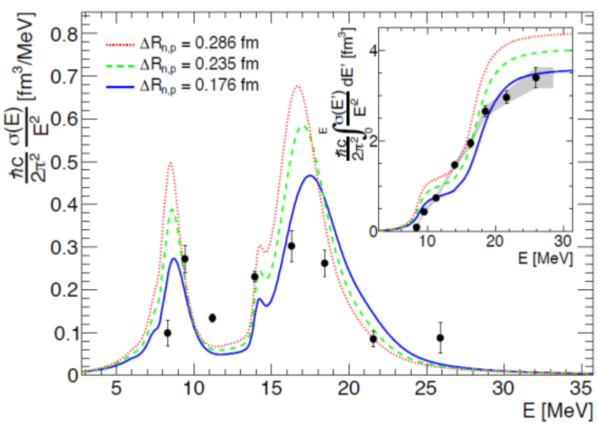

$$\alpha_D = \frac{\hbar c}{2\pi^2}\int_0^\infty \frac{\sigma(E)}{E^2}dE$$

D. Rossi et al.
PRL **111** (2013) 242503

skin thickness ^{68}**Ni**
0.175(21) fm

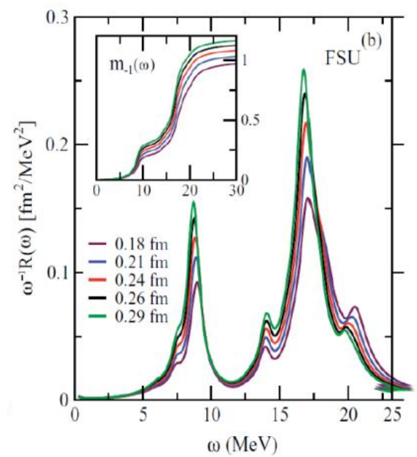

Pb chain & N=126 isotones

~1 A GeV →
bare ions
Fragment identification

J. Piekarewicz, PRC **83** (2011) 034319

The magnet ready
… for travel

- Production
(and revision) finalized.
- FAT passed 23.9.2015

➔„Test bench“ operation
➔Preparation for FAIR

August 2015

September 2015

Transport to GSI
November 2015
SATa Test Q1/2016
Installation Cave-C
Q2/2016
Operation ready
Q1 /2017

GLAD has arrived and is being installed in Cave-C

- Power supply there and tested
- Crypo plant installed and tested
- Magnet has arrived and passed first series of SAT tests

➔ non conformity in the exit flange mitigation in progress

- in-kind contracts with F/D in preparation

- 04/2016 installation of instrumentation and MSS/MCS by CEA
- End 2016 to get magnet into operation!

Next Step: The new FAIR facility

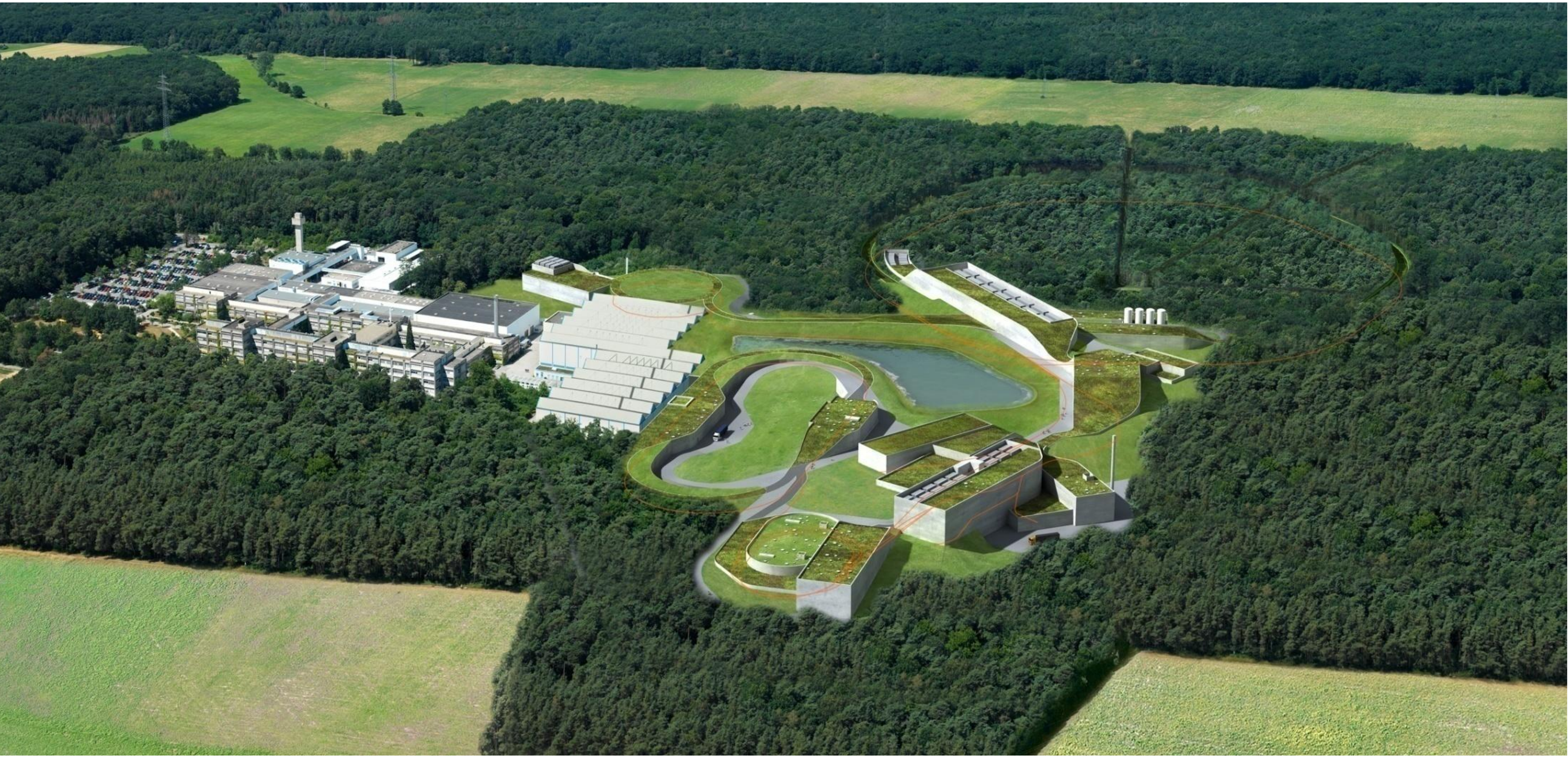

Intensity increase 3-4 orders of magnitude !

The Halo Collaboration

Y. Aksyutina, T. Aumann, H. Álvarez-Pol, T. LeBleis, E. Benjamim, J. Benlliure, K. Boretzky,
M.J.G. Borge, C. Caesar, M.Caamaño, E. Casarejos, L.V. Chulkov, D. Cortina-Gil,
K. Epinger, Th. W. Elze, H. Emling, C. Forssén, H. Geissel, R. Gernhäuser,
M. Hellström, J. Holeczek, K.L. Jones, H. Johansson, B. Jonson, J.V. Kratz, R. Krücken,
R. Kulessa, C.Langer, M. Lantz, Y. Leifels, A. Lindahl, K. Mahata, M. Meister, P. Maierbeck,
K. Markenroth, G. Münzenberg, T. Nilsson, C. Nociforo, G. Nyman, R. Palit, M. Pantea,
S. Paschalis, D.Pérez, M. Pfützner, V. Pribora, A. Prochazka, R. Reifarth, A. Richter,
K. Riisager, C. Rodríguez, C. Scheidenberger, G. Schrieder, H. Simon,
J. Stroth, K. Sümmerer, O. Tengblad, H. Weick, and M.V. Zhukov.

GSI, Darmstadt, Germany; Instito Estructura de la Materia, Madrid, Spain
Kurchatov Institute, Moscow, Russia; Johann-Wolfgang- Goethe-Univ., Frankfurt, Germany;
Chalmers Tekniska Högskola / Göteborgs Universitet, Göteborg, Sweden;
Johannes-Gutenberg-Universität, Mainz, Germany;
Universytet Jagiellonski, Kraków, Poland;
University Santiago de Compostela, Spain;
Technische Universität, Darmstadt, Germany; Technische Universität, München, Germany;
CERN, Genève, Switzerland; Aarhus Universitet, Aarhus, Denmark

The R3B Collaboration

Aksouh, Farouk; Al-Khalili, Jim; Algora, Alejandro; Alkhasov, Georgij; Altstadt, Sebastian; Alvarez, Hector; Atar, Leyla; Audouin, Laurent; Aumann, Thomas; Pellereau, Eric; Martin, Julie-Fiona; Gorbinet, Thomas; Seddon, Dave; Kogimtzis, Mos; Avdeichikov, Vladimir; Barton, Charles; Bayram, Murat; Belier, Gilbert; Bemmerer, Daniel; Michael Bendel; Benlliure, Jose; Bertulani, Carlos; Bhattacharya, Sudeb; Bhattacharya, Chandana; Le Bleis, Tudi; Boilley, David; Boretzky, Konstanze; Borge, Maria Jose; Botvina, Alexander; Boudard, Alain; Boutoux, Guillaume; Boehmer, Michael; Caesar, Christoph; Calvino, Francisco; Casarejos, Enrique; Catford, Wilton; Cederkall, Joakim; Cederwall, Bo; Chapman, Robert; Alexandre Charpy; Chartier, Marielle; Chatillon, Audrey; Chen, Ruofu; Christophe, Mayri; Chulkov, Leonid; Coleman-Smith, Patrick; Cortina, Dolores; Crespo, Raquel; Csatlos, Margit; Cullen, David; Czech, Bronislaw; Danilin, Boris; Davinson, Tom; Paloma Diaz; Dillmann, Iris; Fernandez Dominguez, Beatriz; Ducret, Jean-Eric; Duran, Ignacio; Egelhof, Peter; Elekes, Zoltan; Emling, Hans; Enders, Joachim; Eremin, Vladimir; Ershov, Sergey N.; Ershova, Olga; Eronen, Simo; Estrade, Alfredo; Faestermann, Thomas; Fedorov, Dmitri; Feldmeier, Hans; Le Fevre, Arnaud; Fomichev, Andrey; Forssen, Christian; Freeman, Sean; Freer, Martin; Friese, Juergen; Fynbo, Hans; Gacsi, Zoltan; Garrido, Eduardo; Gasparic, Igor; Gastineau, Bernard; Geissel, Hans; Gelletly, William; Genolini, B.; Gerl, Juergen; Gernhaeuser, Roman; Golovkov, Mikhail; Golubev, Pavel; Grant, Alan; Grigorenko, Leonid; Grosse, Eckart; Gulyas, Janos; Goebel, Kathrin; Gorska, Magdalena; Haas, Oliver Sebastian; Haiduc, Maria; Hasegan, Dumitru; Heftrich, Tanja; Heil, Michael; Heine, Marcel; Heinz, Andreas; Ana Henriques; Hoffmann, Jan; Holl, Matthias; Hunyadi, Matyas; Ignatov, Alexander; Ignatyuk, Anatoly V.; Ilie, Cherciu Madalin; Isaak, Johann; Isaksson, Lennart; Jakobsson, Bo; Jensen, Aksel; Johansen, Jacob; Johansson, Hakan; Johnson, Ron; Jonson, Bjoern; Junghans, Arnd; Jurado, Beatriz; Jaehrling, Simon; Kailas, S.; Kalantar, Nasser; Kalliopuska, Juha; Kanungo, Rituparna; Kelic-Heil, Aleksandra; Kezzar, Khalid; Khanzadeev, Alexei; Kissel, Robert; Kisselev, Oleg; Klimkiewicz, Adam; Kmiecik, Maria; Koerper, Daniel; Kojouharov, Ivan; Korsheninnikov, Alexei; Korten, Wolfram; Krasznahorkay, Attila; Kratz, Jens Volker; Kresan, Dima; Anatoli Krivchitch; Kroell, Thorsten; Krupko, Sergey; Kruecken, Reiner; Kulessa, Reinhard; Kurz, Nikolaus; Kuzmin, Eugenii; Labiche, Marc; Langanke, Karl-Heinz; Langer, Christoph; Lapoux, Valerie; Larsson, Kristian; Laurent, Benoit; Lazarus, Ian; Le, Xuan Chung; Leifels, Yvonne; Lemmon, Roy; Lenske, Horst; Lepine-Szily, Alinka; Leray, Sylvie; Letts, Simon; Li, Songlin; Liang, Xiaoying; Lindberg, Simon; Lindsay, Scott; Litvinov, Yuri; Lukasik, Jerzy; Loeher, Bastian; Mahata, Kripamay; Maj, Adam; Marganiec, Justyna; Meister, Mikael; Mittig, Wolfgang; Movsesyan, Alina; Mutterer, Manfred; Muentz, Christian; Nacher, Enrique; Najafi, Ali; Nakamura, Takashi; Neff, Thomas; Nilsson, Thomas; Nociforo, Chiara; Nolan, Paul; Nolen, Jerry; Nyman, Goran; Obertelli, Alexandre; Obradors, Diego; Ogloblin, Aleksey; Oi, Makito; Palit, Rudrajyoti; Panin, Valerii; Paradela, Carlos; Paschalis, Stefanos; Pawlowski, Piotr; Petri, Marina; Pietralla, Norbert; Pietras, Ben; Pietri, Stephane; Plag, Ralf; Podolyak, Zsolt; Pollacco, Emanuel; Potlog, Mihai; Datta Pramanik, Ushasi; Prasad, Rajeshwari; Fraile Prieto, Luis Mario; Pucknell, Vic; Galaviz -Redondo, Daniel; Regan, Patrick; Reifarth, Rene; Reinhardt, Tobias; Reiter, Peter; Rejmund, Fanny; Ricciardi, Maria Valentina; Richter, Achim; Rigollet, Catherine; Riisager, Karsten; Rodin, Alexander; Rossi, Dominic; Roussel-Chomaz, Patricia; Gonzalez Rozas, Yago; Rubio, Berta; Roeder, Marko; Saito, Takehiko; Salsac, Marie-Delphine; Rodriguez Sanchez, Jose Luis; Santosh, Chakraborty; Savajols, Herve; Savran, Deniz; Scheit, Heiko; Schindler, Fabia; Schmidt, Karl-Heinz; Schmitt, Christelle; Schnorrenberger, Linda; Schrieder, Gerhard; Schrock, Philipp; Sharma, Manoj Kumar; Sherrill, Bradley; Shrivastava, Aradhana; Shulgina, Natalia; Sidorchuk, Sergey; Silva, Joel; Simenel, Cedric; Simon, Haik; Simpson, John; Singh, Pushpendra Pal; Sonnabend, Kerstin; Spohr, Klaus; Stanoiu, Mihai; Stevenson, Paul; Strachan, Jon; Streicher, Brano; Stroth, Joachim; Syndikus, Ina; Suemmerer, Klaus; Taieb, Julien; Tain, Jose L.; Tanihata, Isao; Tashenov, Stanislav; Tassan-Got, Laurent; Tengblad, Olof; Teubig, Pamela; Thies, Ronja; Togano, Yasuhiro; Tostevin, Jeffrey A.; Trautmann, Wolfgang; Tuboltsev, Yuri; Turrion, Manuela; Typel, Stefan; Udias-Moinelo, Jose; Vaagen, Jan; Velho, Paulo; Verbitskaya, Elena; Veselsky, Martin; Wagner, Andreas; Walus, Wladyslaw; Wamers, Felix; Weick, Helmut; Wimmer, Christine; Winfield, John; Winkler, Martin; Woods, Phil; Xu, Hushan; Yakorev, Dmitry; Zegers, Remco; Zhang, Yu-Hu; Zhukov, Mikhail; Zieblinski, Miroslaw; Zilges, Andreas;

Incredients for the ^{7}H case

- t + n + n + n + n

PHYSICAL REVIEW C 77, 054317 (2008)

Strong dineutron correlation in ^{8}He and ^{18}C

K. Hagino,[1] N. Takahashi,[1] and H. Sagawa[2]

Core +4n (HFB)

PHYSICAL REVIEW C 80, 021304(R) (2009)

Di-neutron correlations in ^{7}H

S. Aoyama[1] and N. Itagaki[2]

Core +4n
AMD selected snapshots

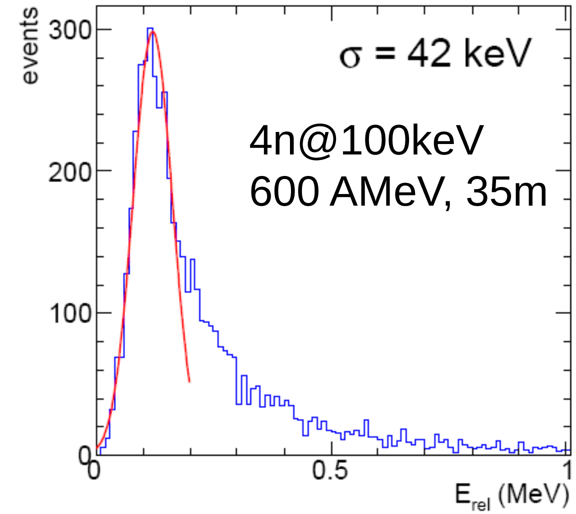

NeuLAND Simul.

- t + 2n + 2n

^{11}Li - α → ^{7}H + 2n + 2n
^{8}He – p → ^{7}H + 2n + 2n

➔ Analysis of three body correlations

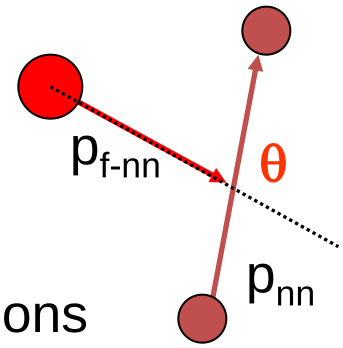

Current experimental frontiers:

^{24}F	^{25}F	^{26}F	^{27}F	^{28}F	^{29}F
0.34 s	50 ms	10.2 ms	4.9 ms	unbound	2.6 ms
^{23}O	^{24}O	^{25}O	^{26}O		
82 ms	61 ms	unbound	unbound		

Low energy response

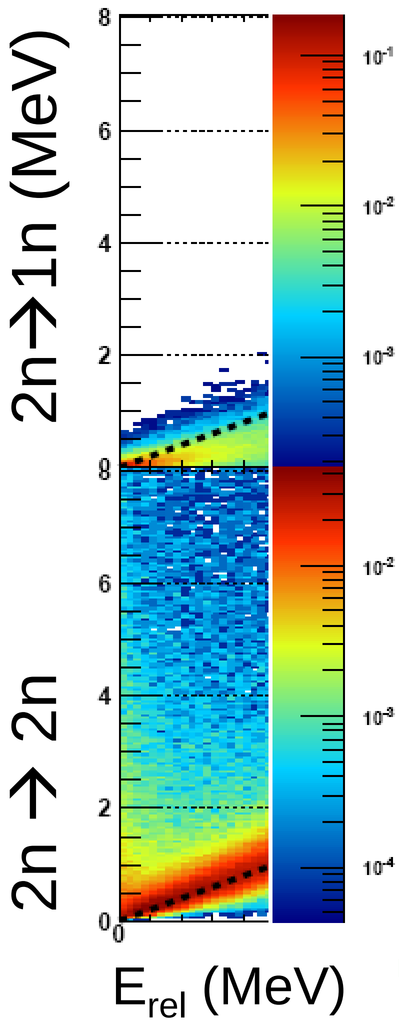

1) Beam intensity

2) Multi neutron detection and acceptance.

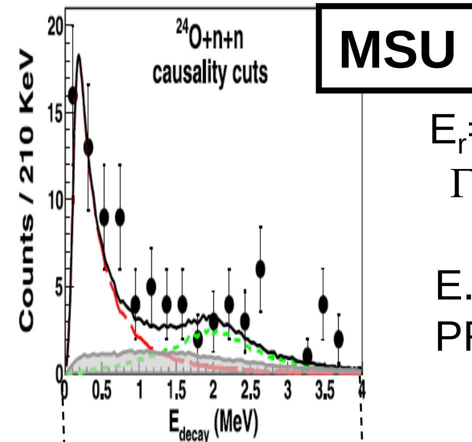

$E_r = 150^{+50}_{-150}$ keV
$\Gamma = 5$ keV

E. Lunderberg et al. PRL108(2012) 142503

Thesis: C.Cäsar TUD/GSI

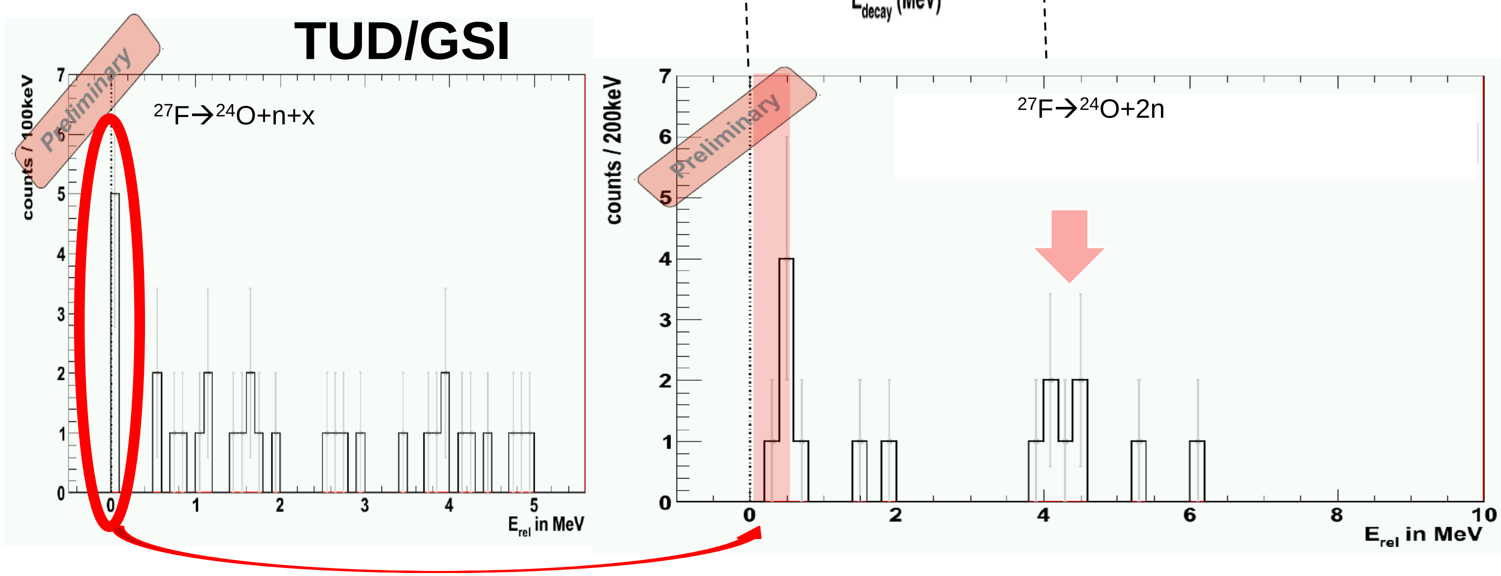

Beyond the dripline: ^{7}H (just) missing mass spectra

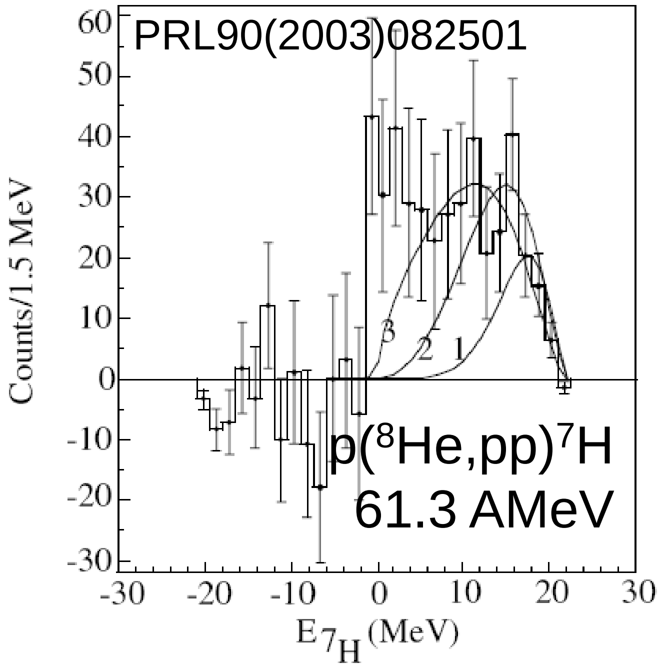

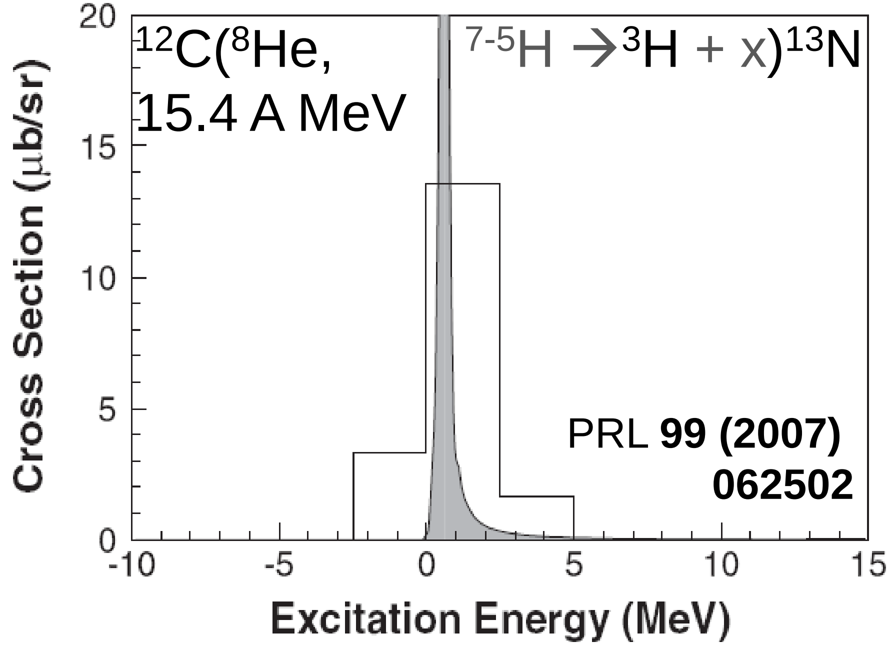

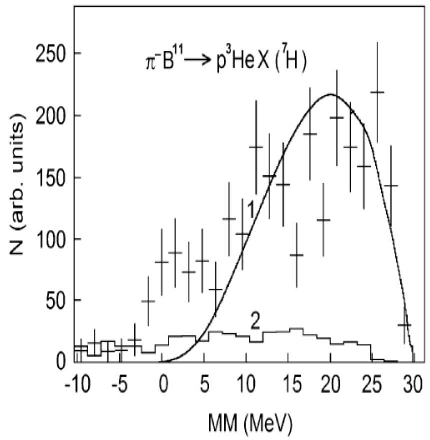

EPJA 32 (2007) 261

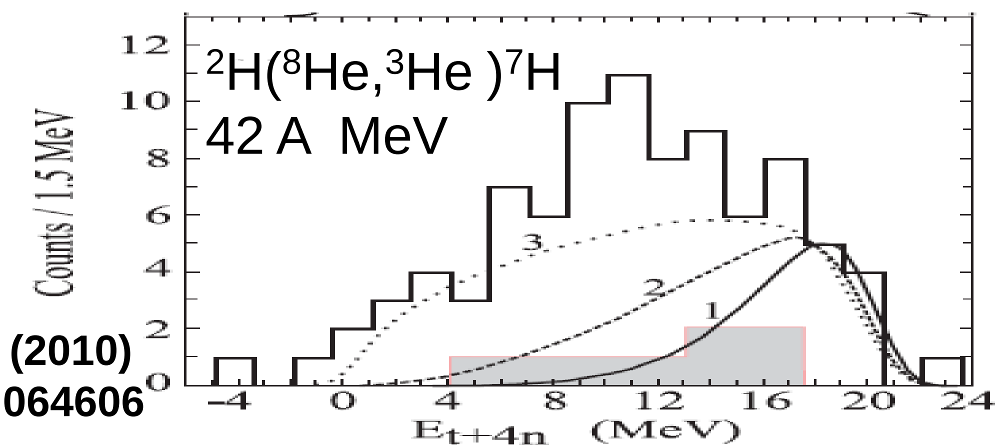

PRC81 **(2010) 064606**

Beyond the dripline: ^{5}H (just) energy spectra

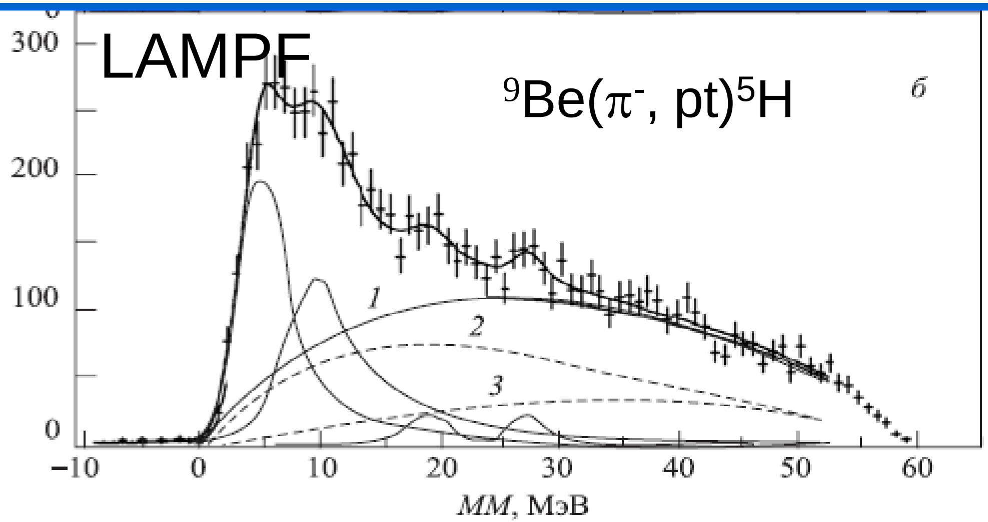

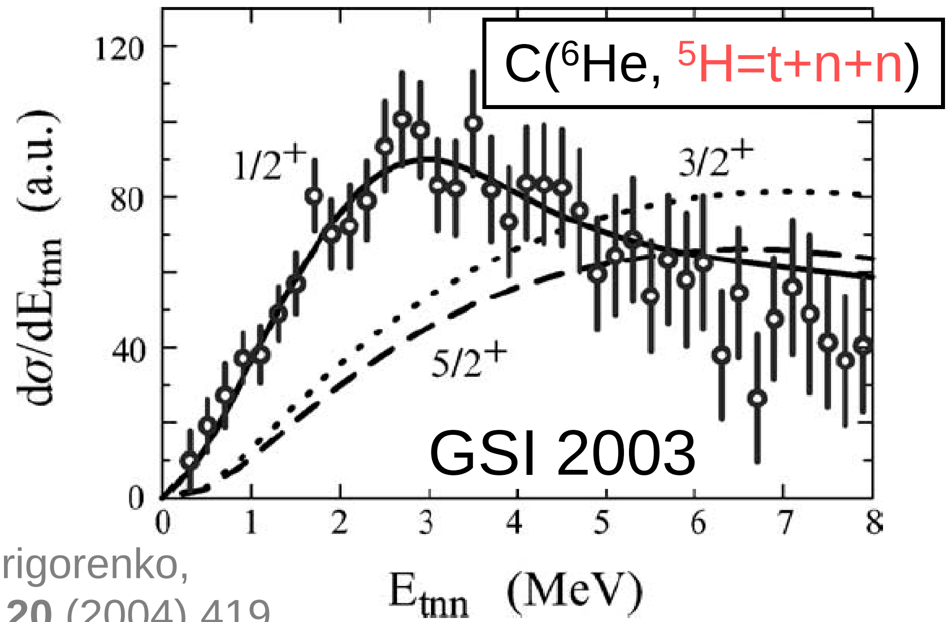

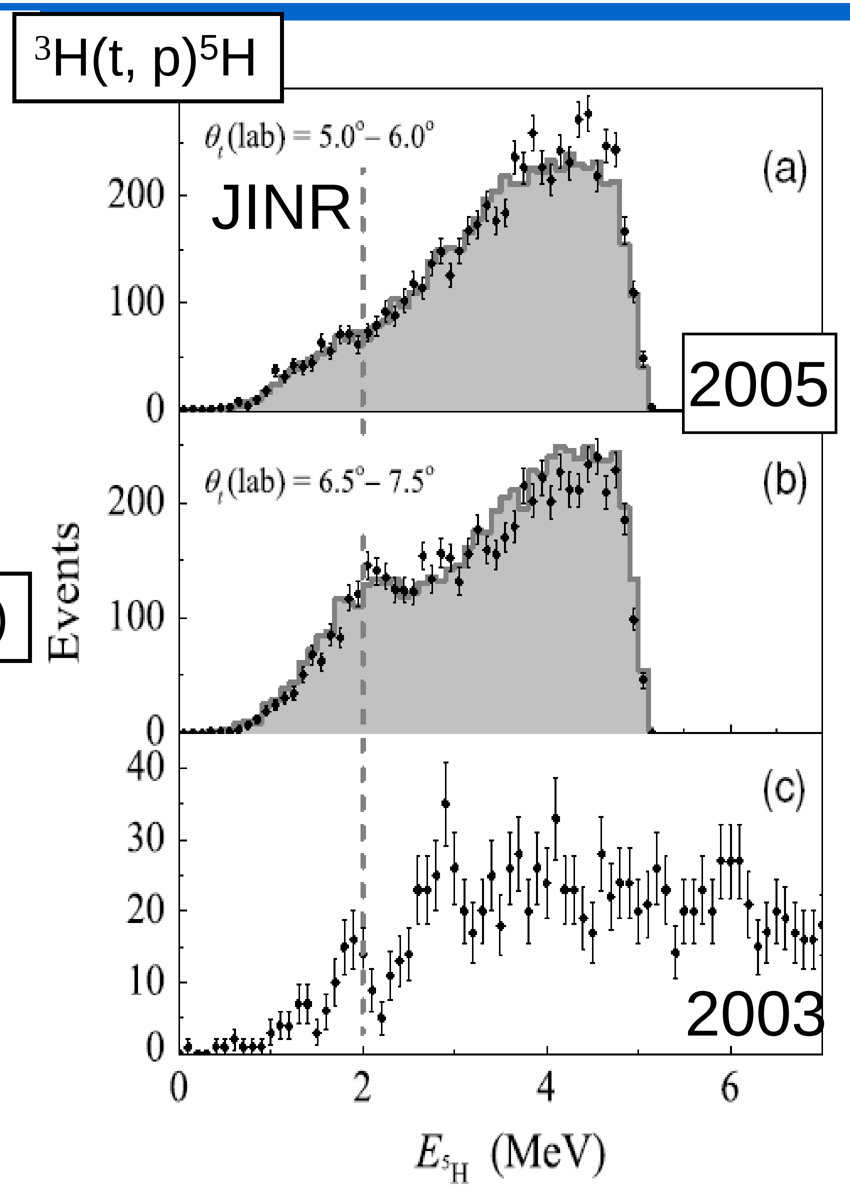

➔L. Grigorenko,
EPJ **A 20** (2004) 419

Beyond the dripline: ^{5}H interpretation

^{6}He

^{5}H

R. de Diego, et al.
Nucl. Phys. **A786**(2007)71

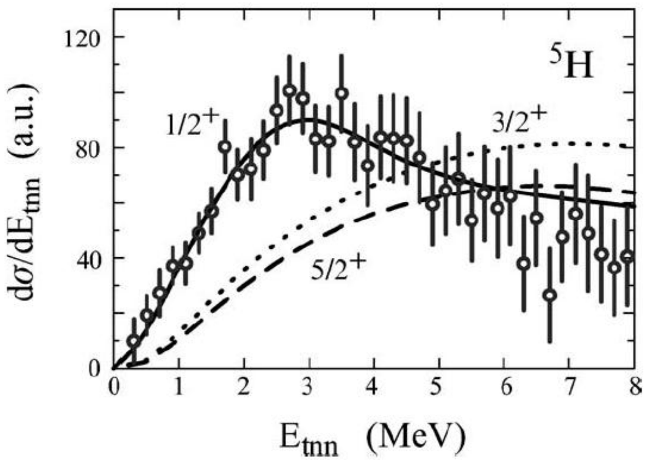

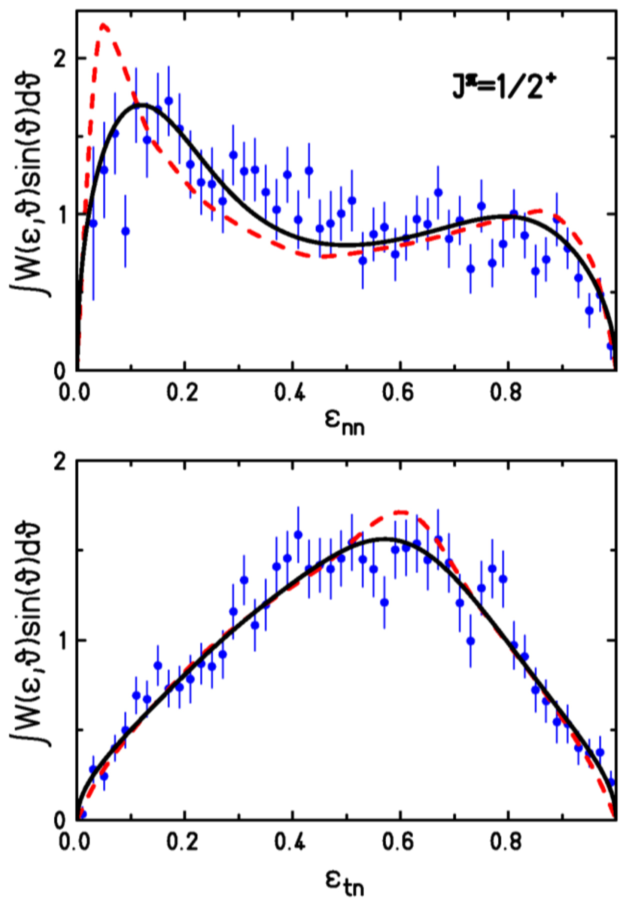

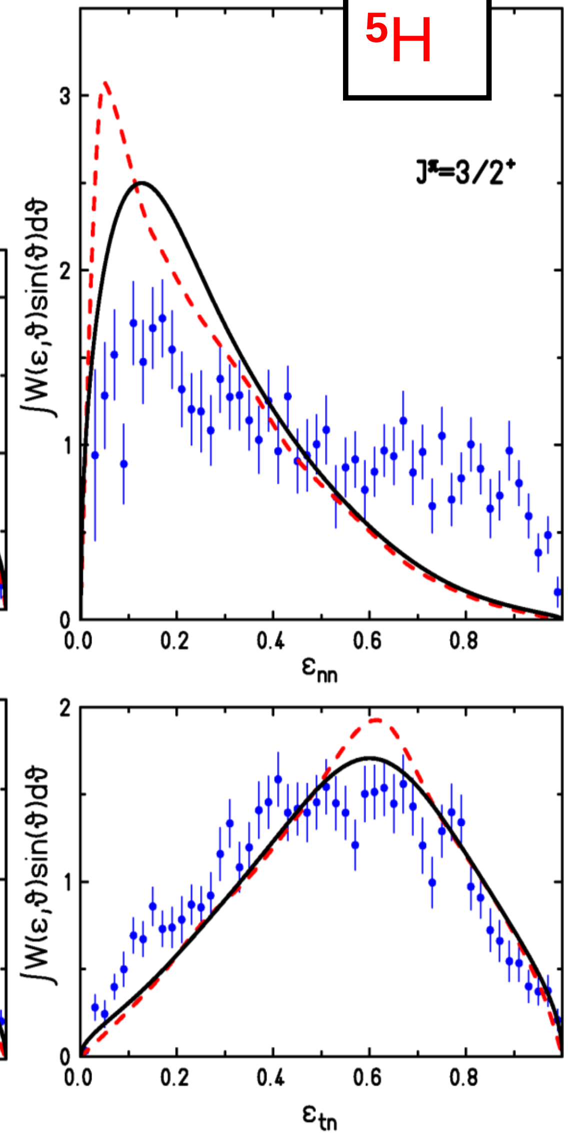

Data:

Nucl. Phys. **A723** (2003) 13

Microscopic calculation:

Phys. Rev. **C62** (2000) 014312


GSI-MAGAZIN
target
Ausgabe Nr. 12
September 2014
GSI Helmholtzzentrum für Schwerionenforschung
Neutronen enttarnen mit NeuLAND
Wie sind sehr neutronenreiche Kerne aufgebaut? Um dieser Frage nachzugehen bauen Forscher den Neutronendetektor NeuLAND. NeuLAND wird am zukünftigen Teilchenbeschleuniger FAIR eingesetzt. Das Ziel: Die Elemententstehung in Supernovae entschlüsseln.
Lesen Sie mehr auf Seite 11
HELMHOLTZ
GEMEINSCHAFT

Next Step: Novel neutron detector for R^3B - NeuLAND demonstrator performance

6 Double planes in test (August and October 2014)

(full detector 30)

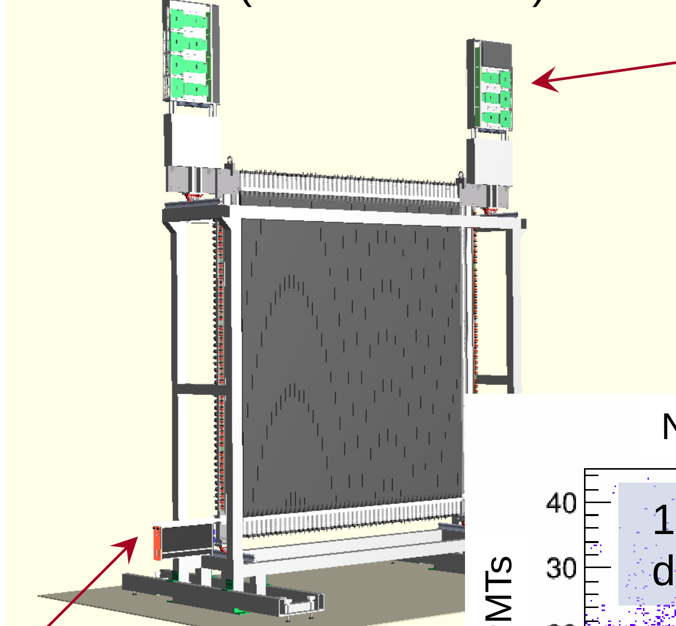

FPGA TDC based

Readout Electronics

HV system

PNPI: Site Acceptance Test week before X-Mas 2014

Neutron hit patterns in 4 double planes

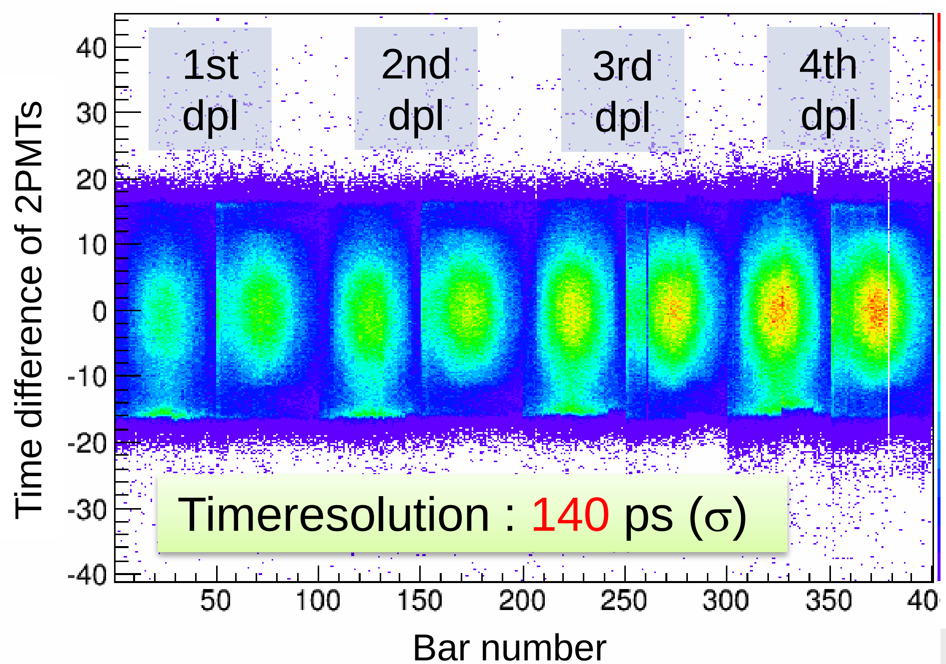

Improve multi neutron detection efficiency down to low energy

Next step:
R^3B Time-of-flight detector prototyping

Performance goals:

- Time resolution σ_t/t = 2E-4
  (⇔ σ_t =20 ps for 20 m flight path at 1 *A*GeV)
- Energy resolution σ_E /E = 1%
- High-counting rate capabilities (~1 MHz)
- Large dynamic range (up to Pb-U).
- FPGA based TDC readout (ΔE via ToT Techniques)

Detector layout

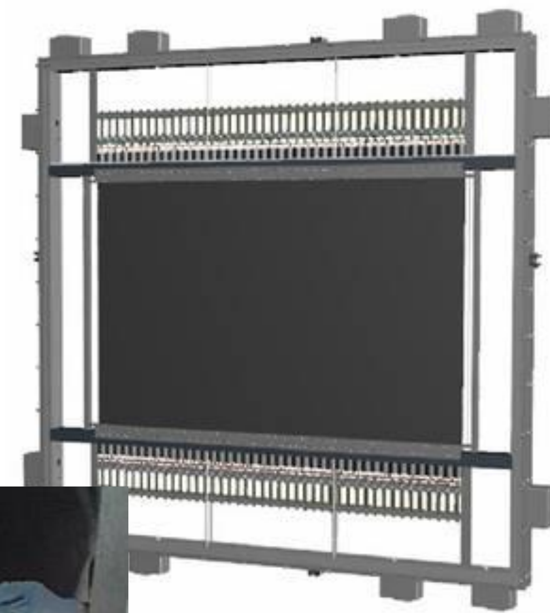

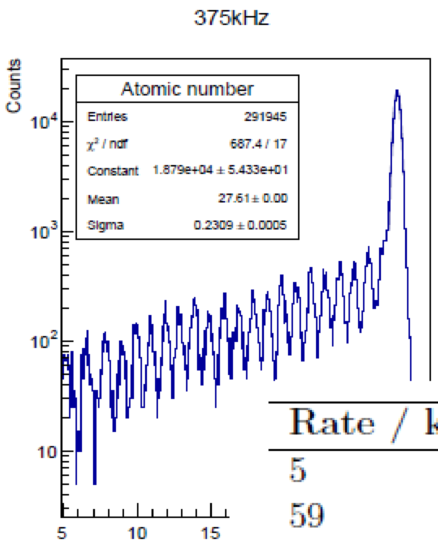

Excellent time and energy resolution at high rates

Rate / kHz	σ_t / ps	σ_t^{det} / ps
5	41	14
59	41	14
375	45	16
1000	64	23

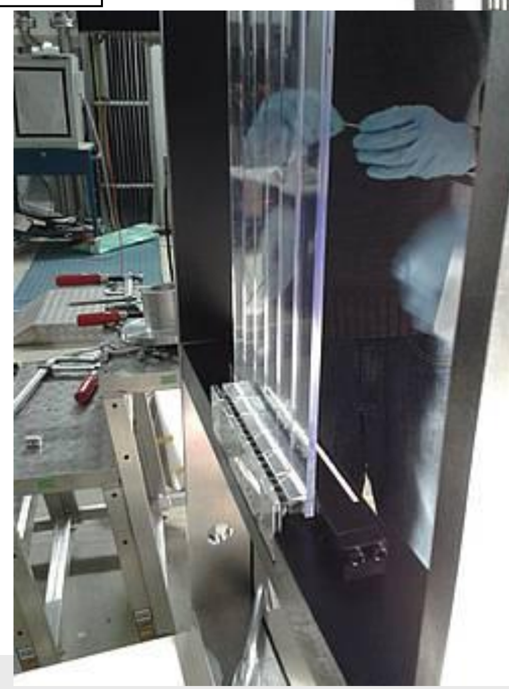

Prototype studies @ Cave-C 08/2014 10/2014

2013/14

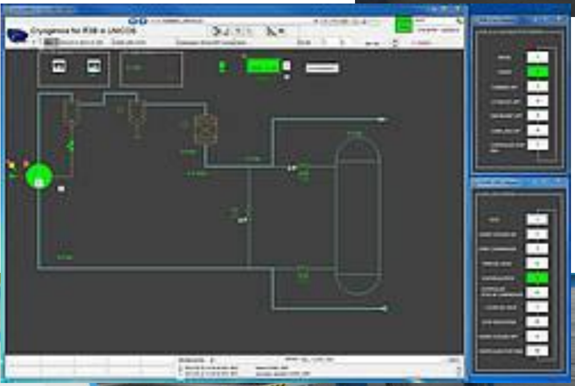

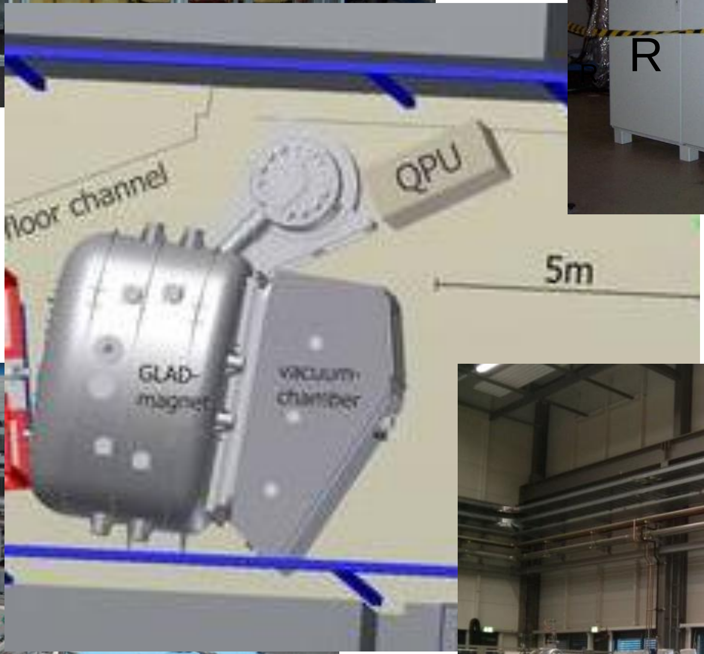

First setup of principal components @ GSI

The structure of ^{11}Li via ^{10}Li

^{10}Li	^{11}Li

^{11}Li + C → ^{9}Li +n + x

a_s =-30 $^{+12}_{-31}$ fm
E*=0.51(44) MeV
Γ =0.54(16) MeV

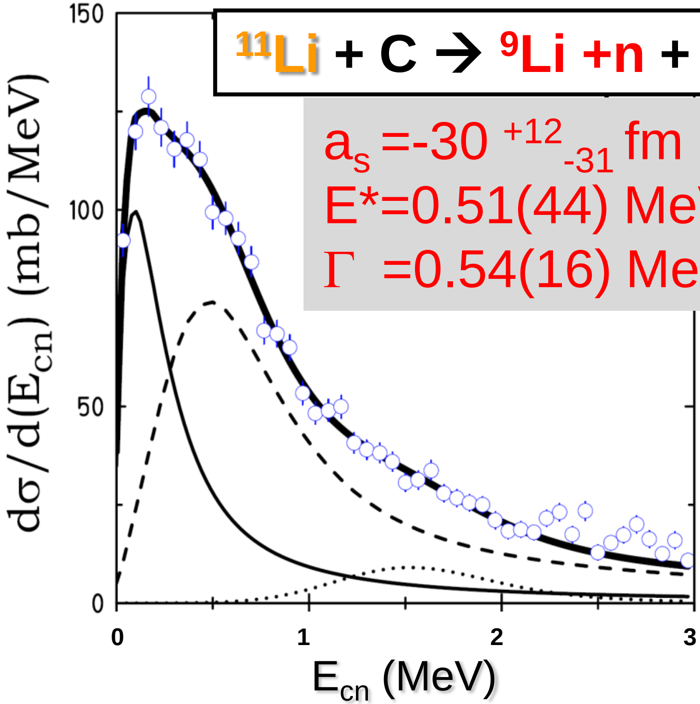

H.S. et al.
Phys. Rev. Lett. **83** (1999) 496
Nucl. Phys. **A 791** (2007) 267

Confirmed eg @ GANIL (N.Orr, H.Al Falou)
^{11}Be, ^{14,15}B → ^{9}Li+n

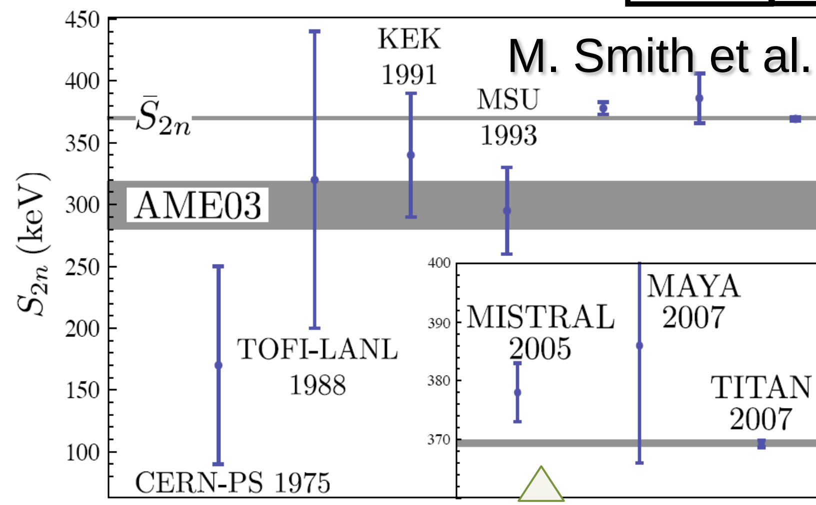

PRL **101,** 202501 (2008) Nucl.Phys.**A826,** 1 (2009)

Correlation data, B(E1), matter radii, cross sections
binding energy 369.15(65) keV
charge radius 2.467(37) fm
R. Sanchez et al., PRL**96** (2006) 033002
quadrupole moment 33.3 (5) mb
R. Neugart et al., PRL**101**(2008)132502

Phenomenological wave function
N.B. Shulgina, B. Jonson, M.V.Zhukov
Nucl. Phys. **A825**(2009)175

$(s1/2)^2$: 37%
$(p1/2)^2$: 47%
$(p3/2)^2$: 9%

Possible similarity of ^{10}He and ^{11}Li g.s.

^{11}Li
^{10}He

Shigeyoshi Aoyama, PRL**89** (2002) 052501

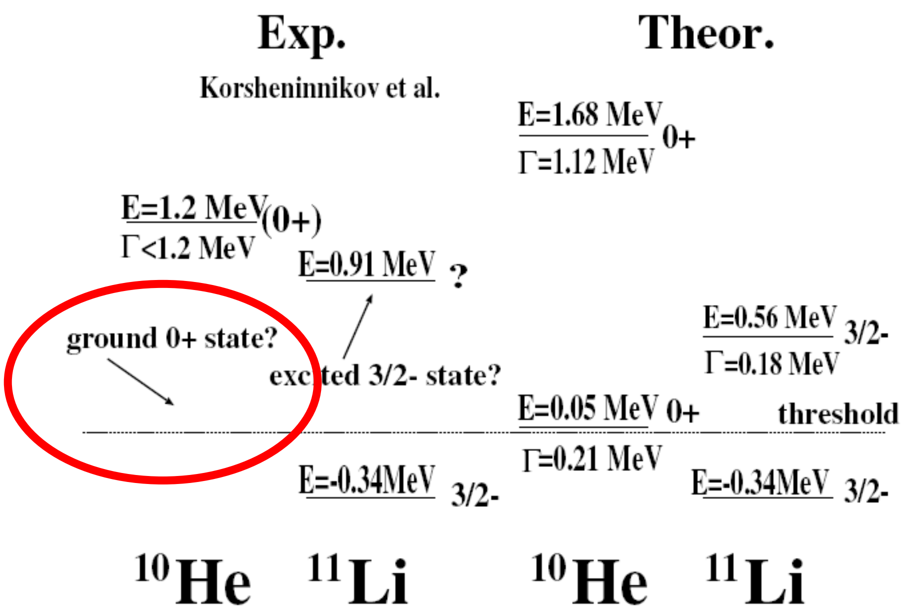

^{11}Li + p/CD_2,C → ^{8}He + n + n

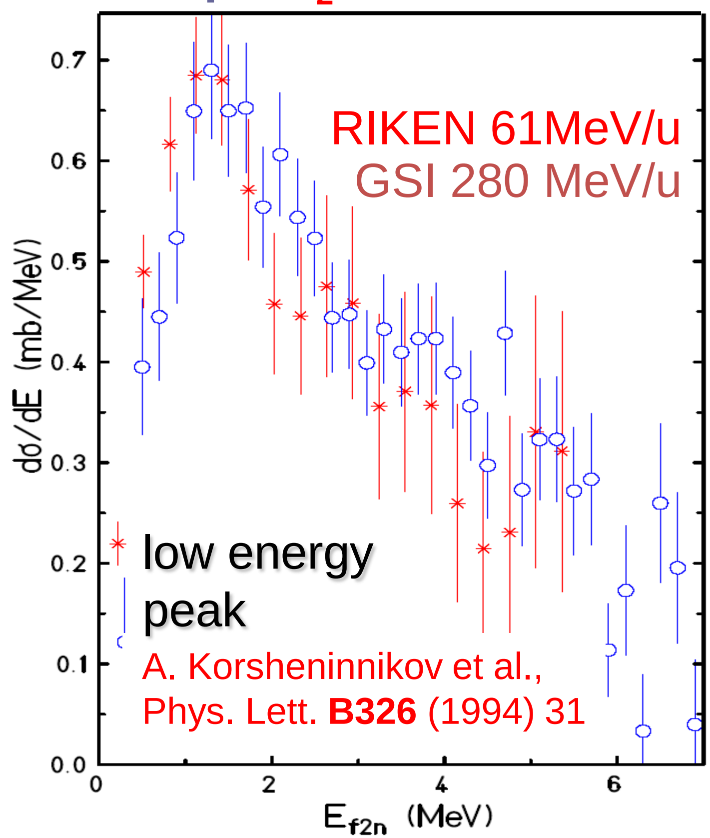

^{10}He: Lowest peak @~1.6 MeV confirmed:

^{14}Be-2p2n@NSCL: PRL 109, 232501 **(2012)**

\+ **Efficiency@small relative neutron energies !**

^{14}Be-2p2n@NSCL: PRC **91, 044312 (2015)**

^{11}Li: Kanungo et al .,Triumf: **3/2+ isoscalar** @ 1 MeV PRL 114, 192502 (2015)

Groundstate properties of ^{9}He (→ ^{10}He)
- different seed nuclei & transfer

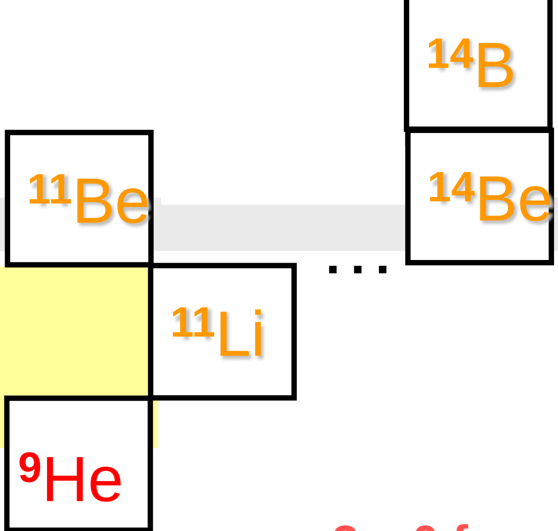

E_r=1.33(8) MeV, Γ=0.1 MeV
E_r=2.4 MeV, Γ=0.7 MeV
Prog.Part. Nucl.Phys. 42(1999)17

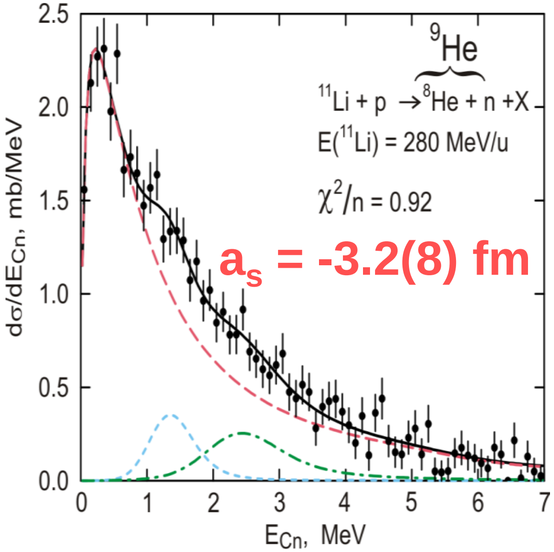

H.T. Johansson et al., Nucl. Phys. **A842** (2010) 15

GANIL

a_s = - 3 .. 0 fm

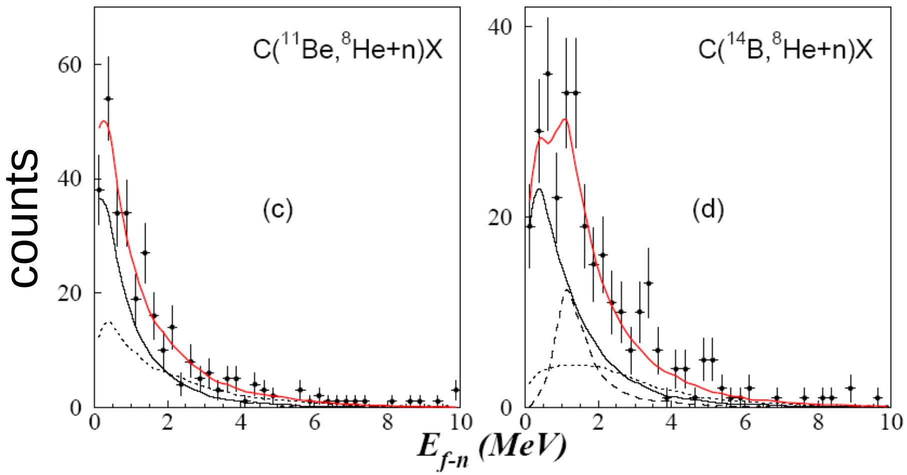

A. Falouh et al., Niigata Conf. 2010
T. al Kalanee et al.PRC **88** (2013) 034301
a_s ~10-12 fm ^{8}He(d,p) @15.4 MeV/u

M.D. Jones et al., PRC **91, 044312 (2015)**

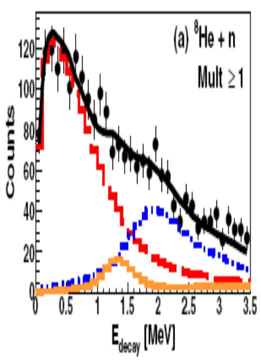

Nucleus	J^π	E (MeV)	Γ (MeV)
^{9}He	$1/2^+$	−3 fm[a] [4]	8.4 [4]
	$1/2^-$	1.33 [4,14]	0.1 [14]
	$3/2^-$	$1.9^{+0.4}_{-0.2}$ †	0.7 [14]

Anomalous population of ^{10}He states in reactions with ^{11}Li

P.G. Sharov,[1,2] I.A. Egorova,[3,2] and L.V. Grigorenko[1,4,5]

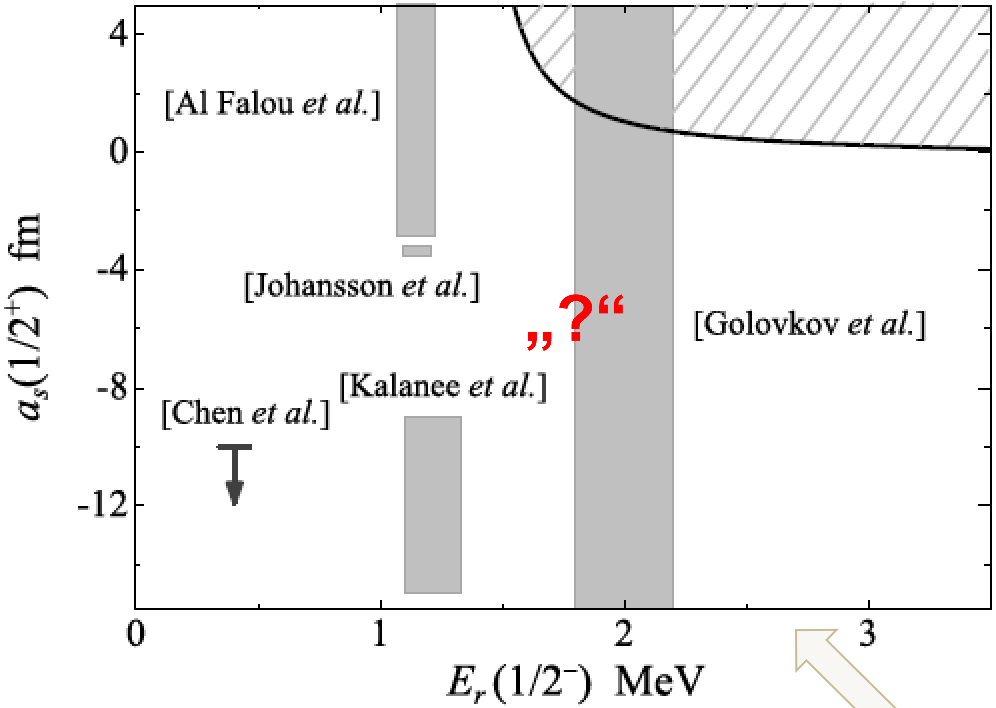

Prediction for ^{9}He states
Using a calculation for the ^{10}He ground state

Missing Mass ^{9}He
PRC76(2007)021605

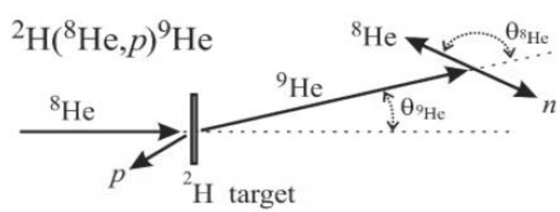

25MeV/u

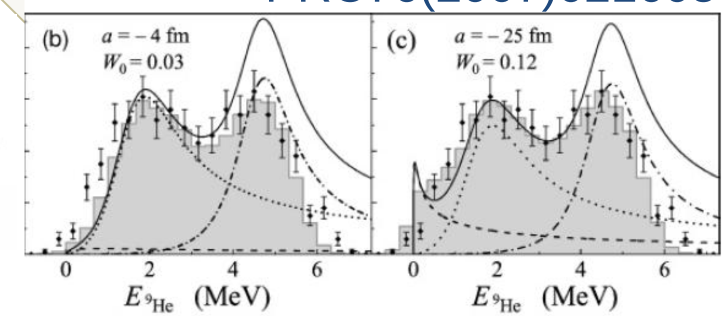

Comparison ^{11}Li and ^{10}He via angular correlations

^{11}Li

^{9}He

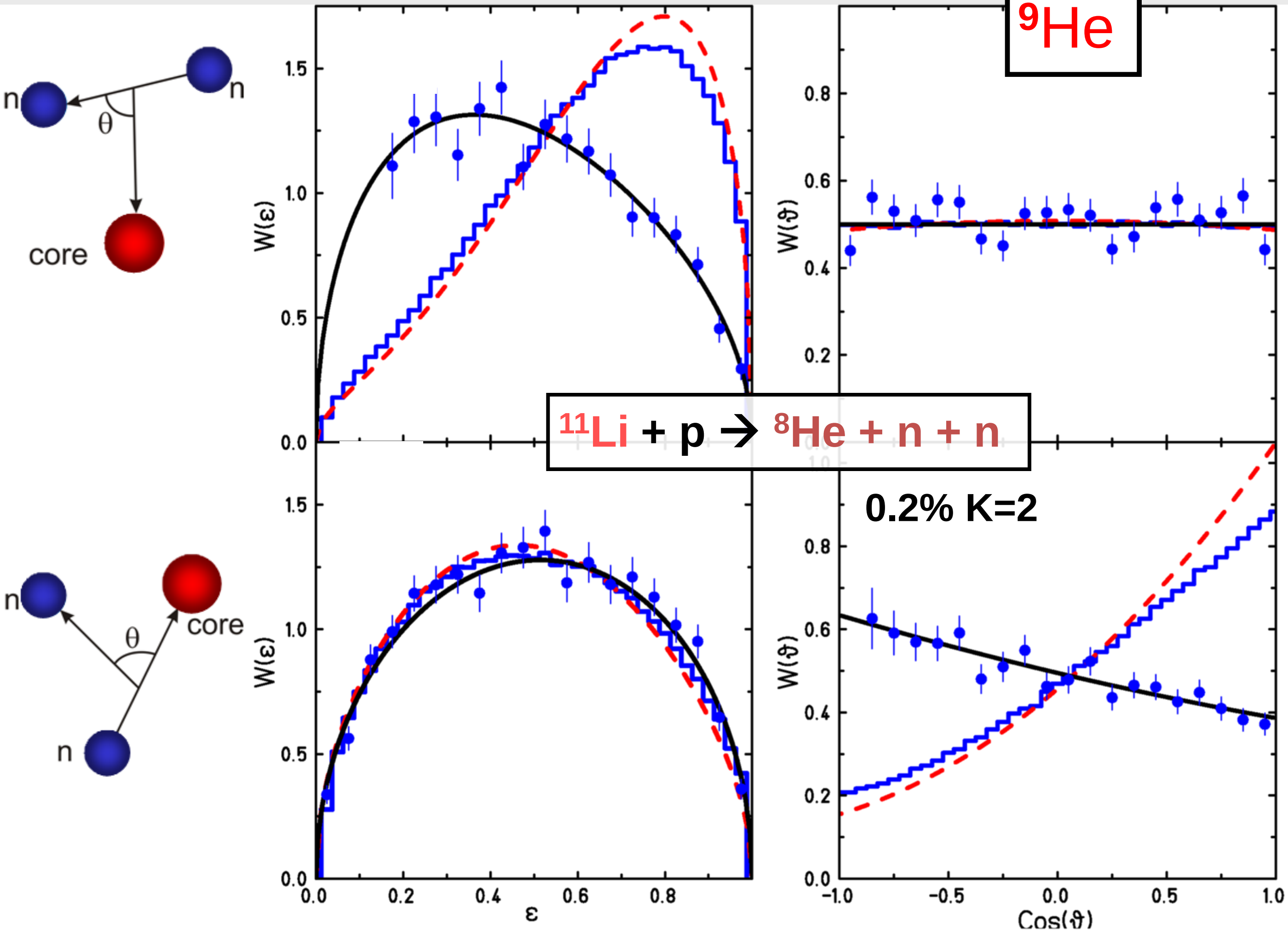

Excitation energy range 1-3 MeV (low energy region 0^{+})

above 2+

- no resemblance to ^{11}Li seed angular correlations

→ ^{10}He is structurally different

H.T. Johansson, Y. Aksyutina, Nucl. Phys. **A847** (2010) 66

^{11}Li wave function → Correlation → Experimental Filter

Anomalous population of ^{10}He states in reactions with ^{11}Li

P.G. Sharov,[1,2] I.A. Egorova,[3,2] and L.V. Grigorenko[1,4,5]

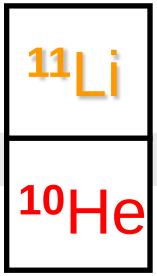

transfer

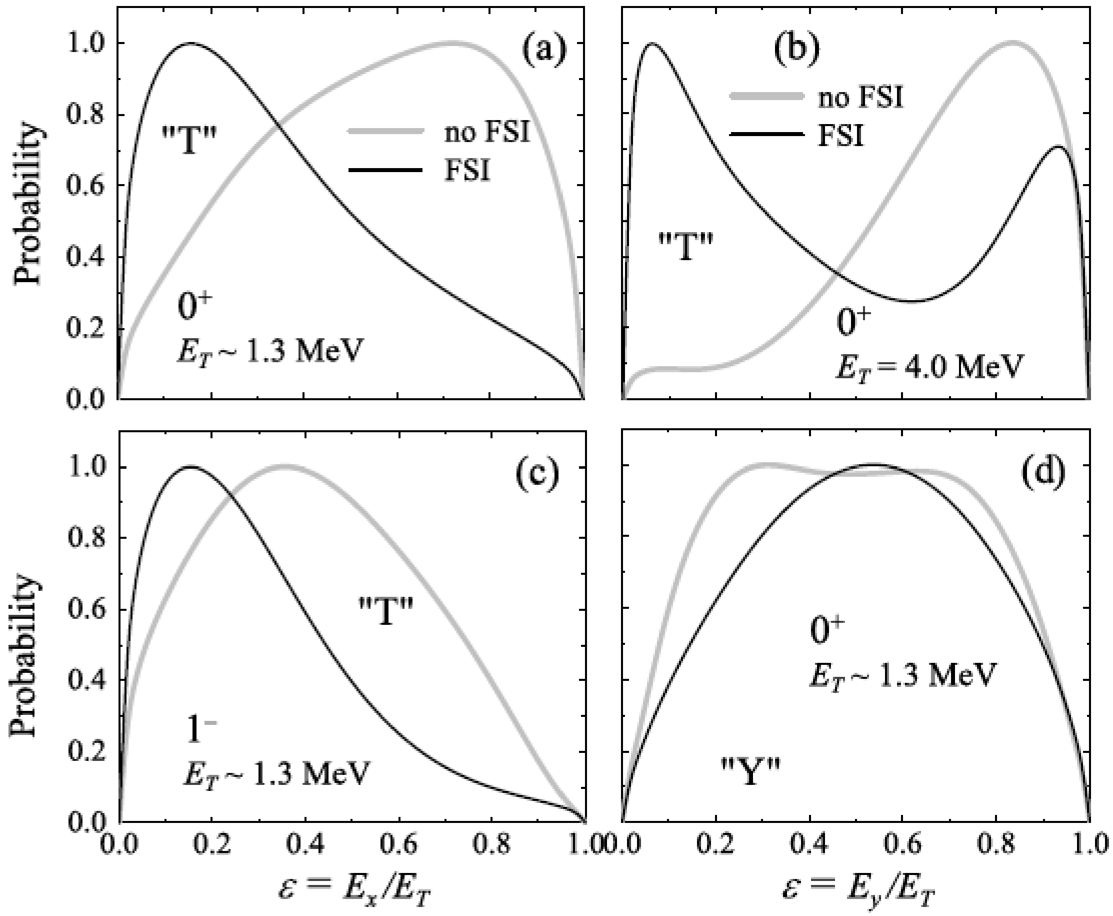

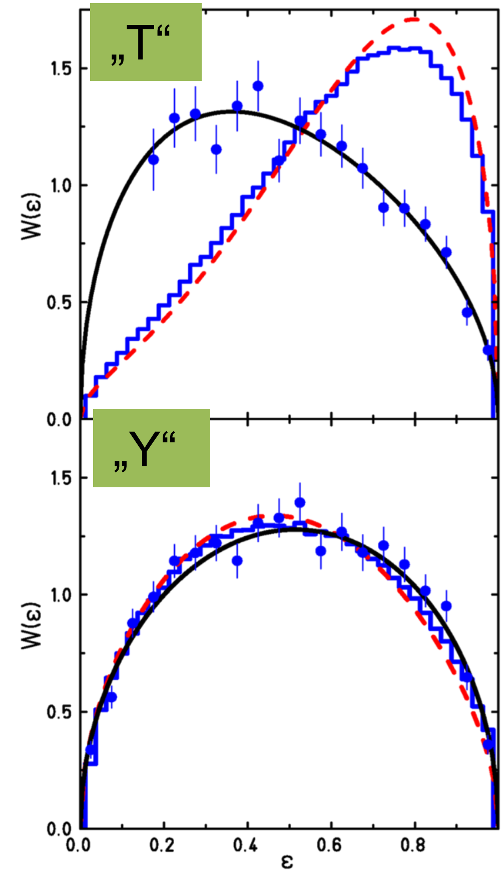

1. ^{10}He FSI modifies strongly the initial correlations.
2. Deviations from our data …

Theory <meets> Experiment ^{10}He groundstate

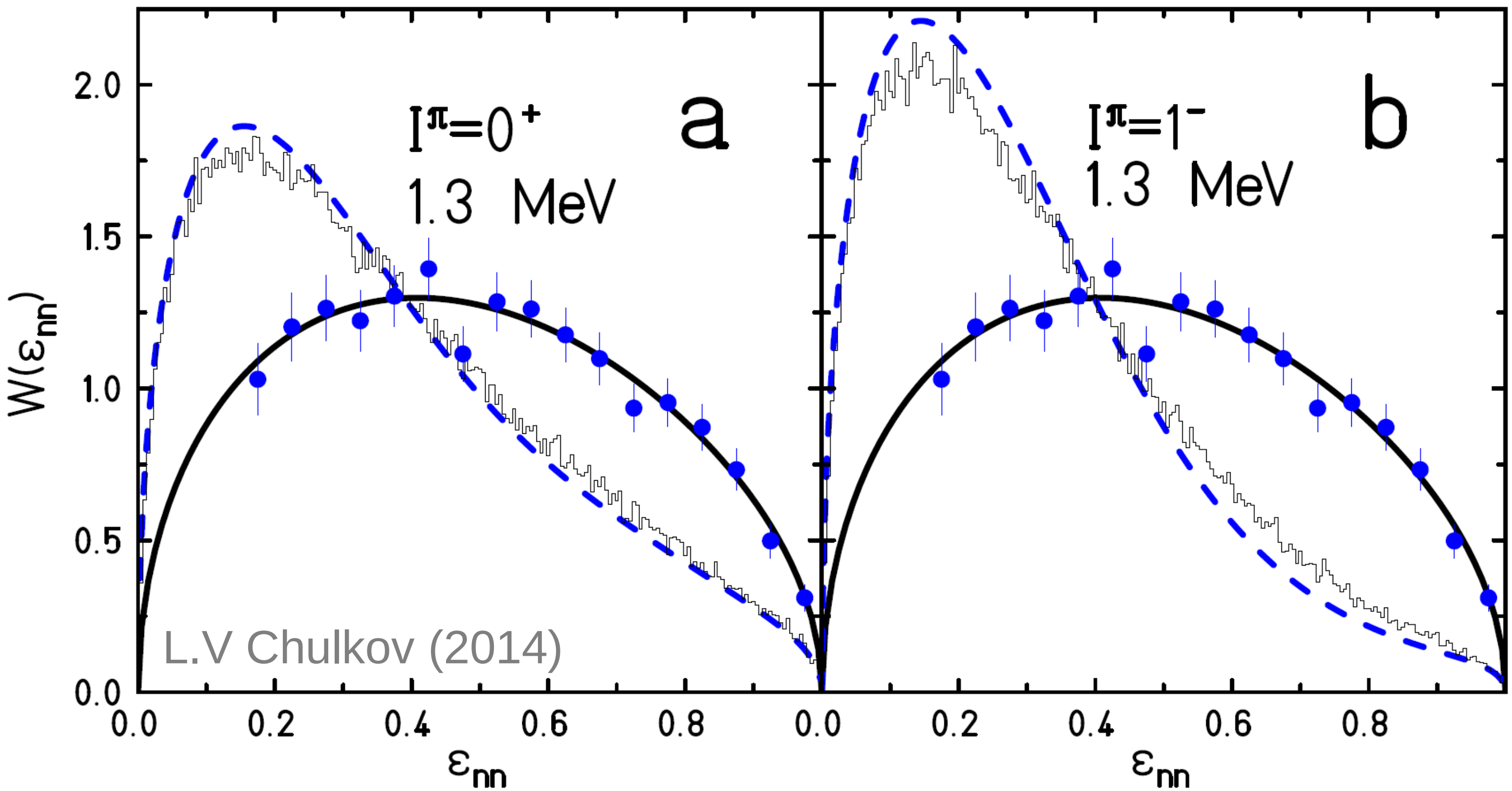

… cannot be explained by experimental effects

➔ No conclusive evidence for a low lying 1^- state.
accordance to H.T.Fortune PRC88 (2013)034328

Linking seed nucleus with intermediate system
- angular correlations vs. relative energy

^{10}Li ^{11}Li

Polynomial fit

A + B cos(θ) + C cos²(θ)

for angular correlations

Plot parameters vs. ^{10}Li relative energy spectrum

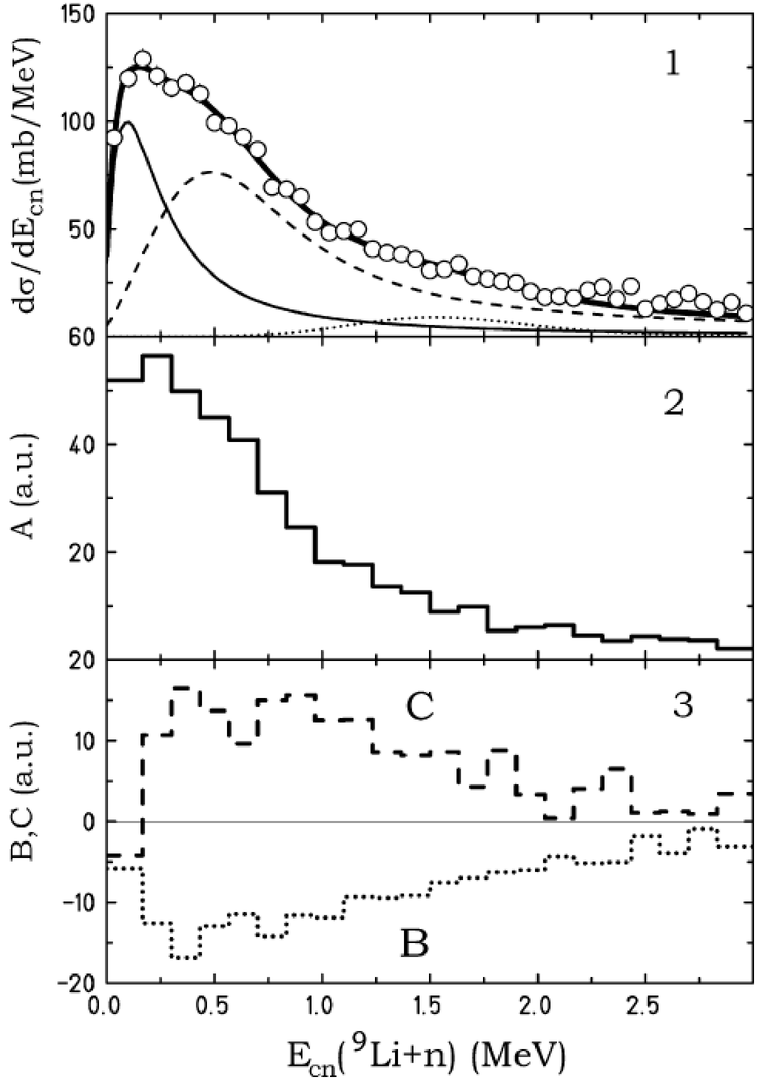

➔s @ threshold
➔p @ ~ 0.5 MeV

H.S. et al., NPA791 (2007) 267

Excitation spectrum ^{10}He* JINR/ACCULINA

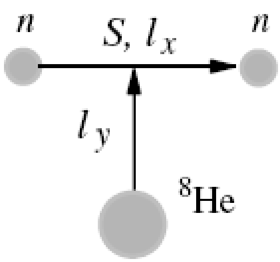

S.I. Sidorchuk et al.
PRL 108(2012)202502
^{3}H(^{8}He,p)^{10}He @21.5AMeV

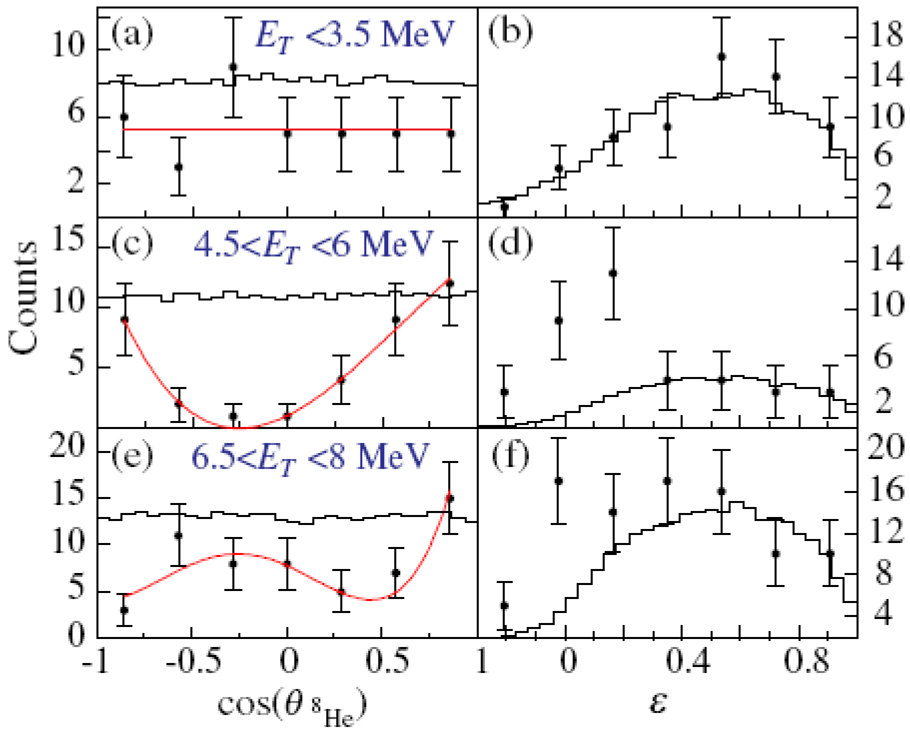

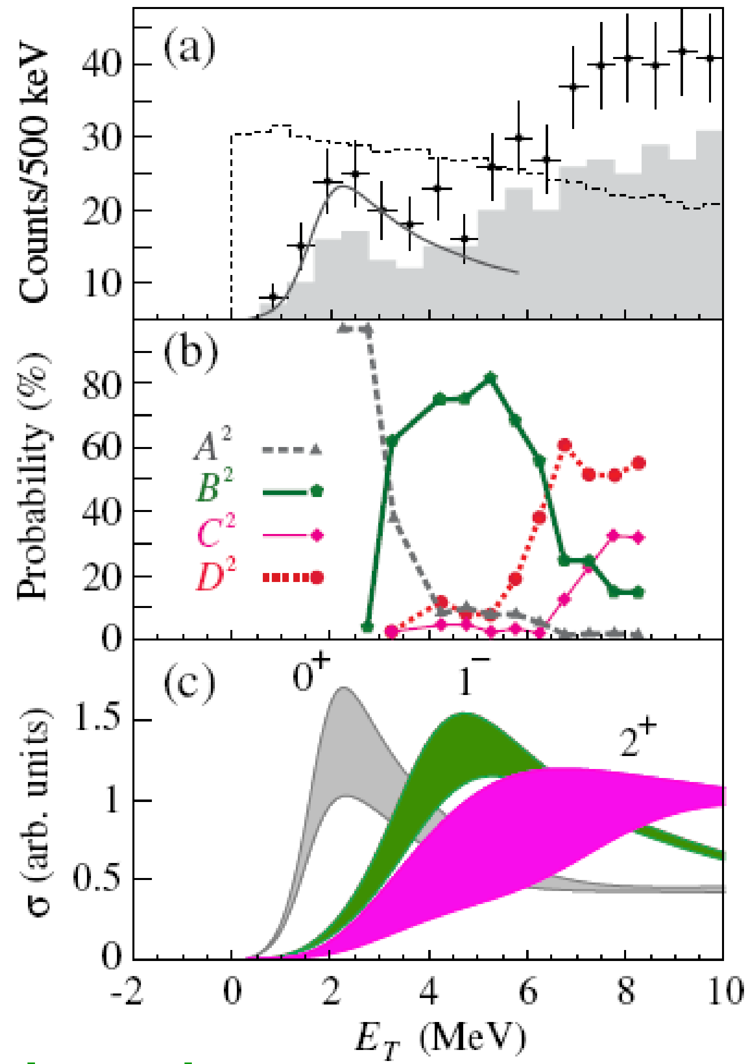

Indication for soft dipole mode

Theory <meets> Experiment $^{10}He^{*}$ excited

^{11}Li

^{10}He

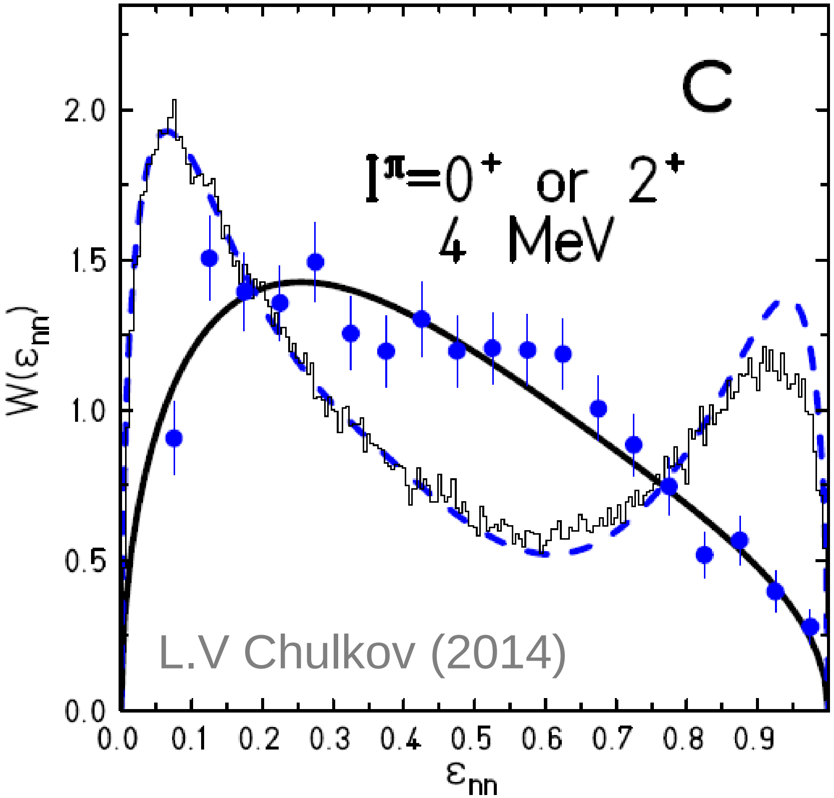

… as well not at higher energies

➔ Direct discussion ongoing !

Lessons learned:

1. Initial state and final state can be separated by measuring the correlations in the system.
2. The energy spectra are strongly influenced by the initial state and the reaction mechanism.
3. Data sets are otherwise often consistent.
4. Interplay with theory – including structure and reaction theory is needed!

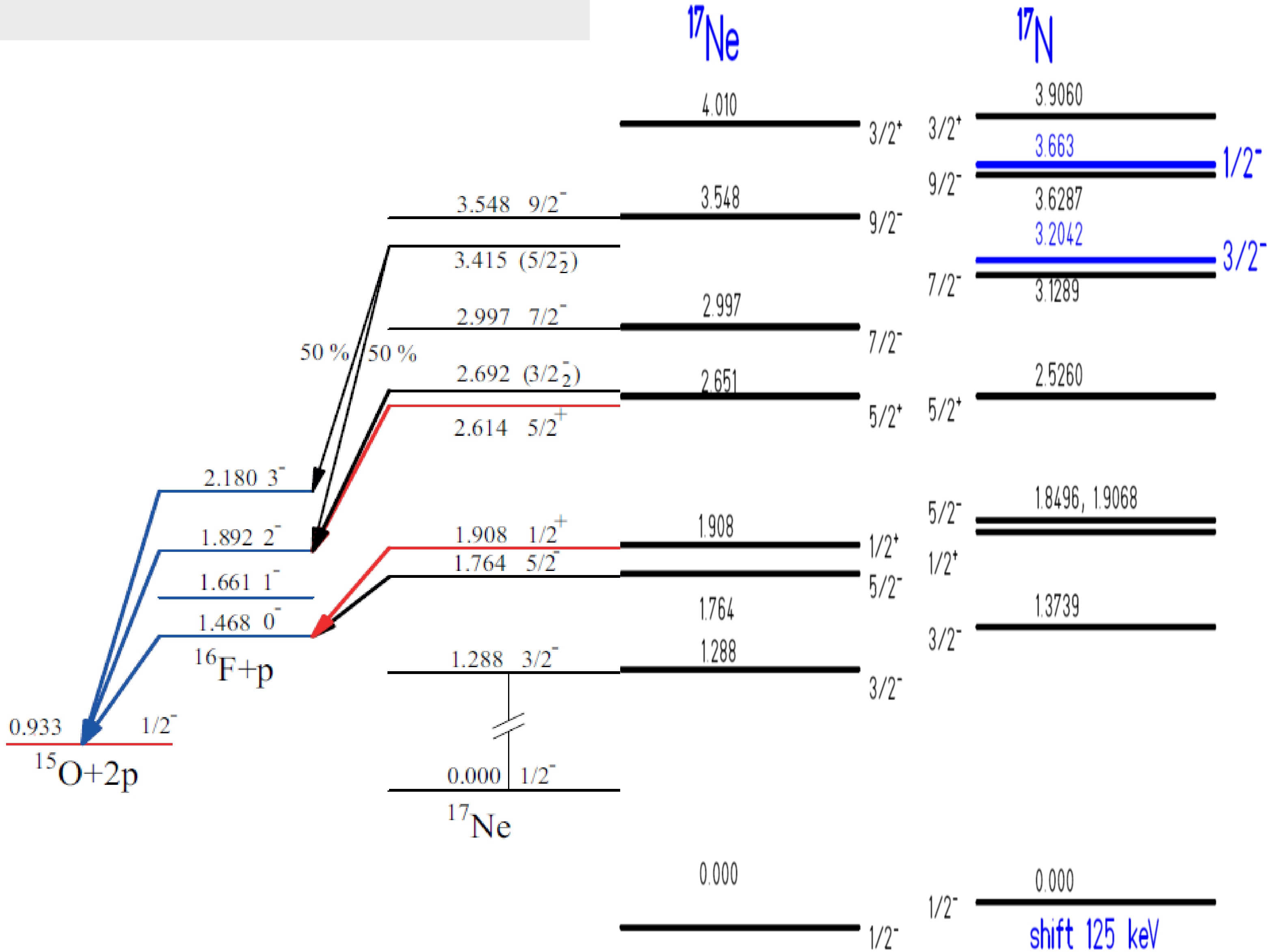

17Ne
17N
4.010
3/2+
3.9060
3/2+
3.663
1/2-
9/2-
3.6287
3.2042
3/2-
7/2-
3.1289
3.548 9/2-
3.548
9/2-
3.415 (5/2-2)
2.997 7/2-
2.997
7/2-
50 %
50 %
2.692 (3/2-2)
2.651
5/2+
5/2+
2.5260
2.614 5/2+
2.180 3-
1.892 2-
1.908 1/2+
1.908
1/2+
5/2-
1.8496, 1.9068
1/2+
1.764 5/2-
5/2-
1.661 1-
1.764
1.3739
1.468 0-
16F+p
3/2-
1.288 3/2-
1.288
3/2-
0.933
1/2-
15O+2p
0.000 1/2-
17Ne
0.000
0.000
1/2-
1/2-
shift 125 keV

Neutron Knockout from ^{17}Ne: Unbound ^{16}Ne

F. Wamers

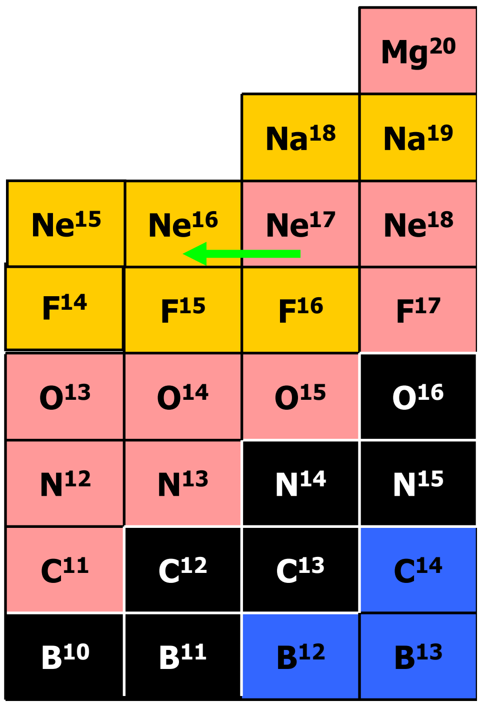

One-neutron Knockout

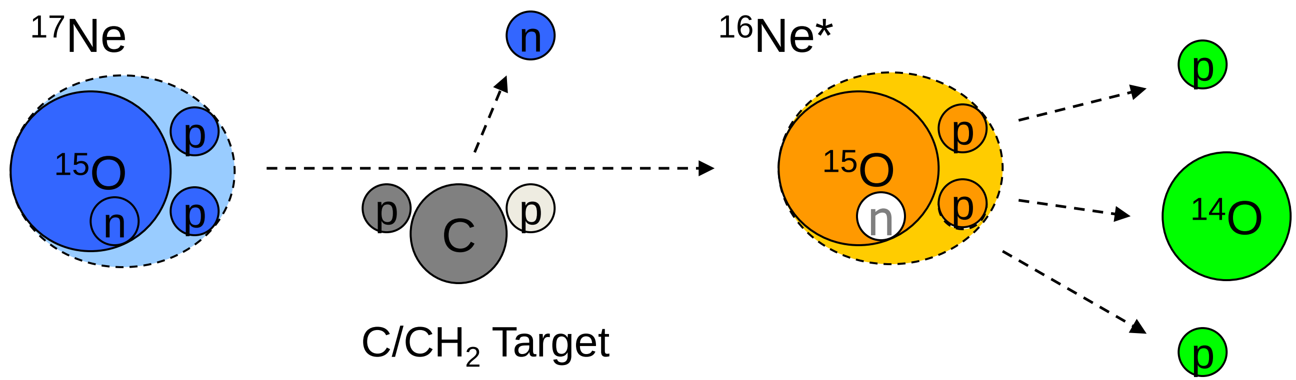

^{16}Ne relative energy spectrum

F. Wamers et al., PRL 112, 132502 (2014)

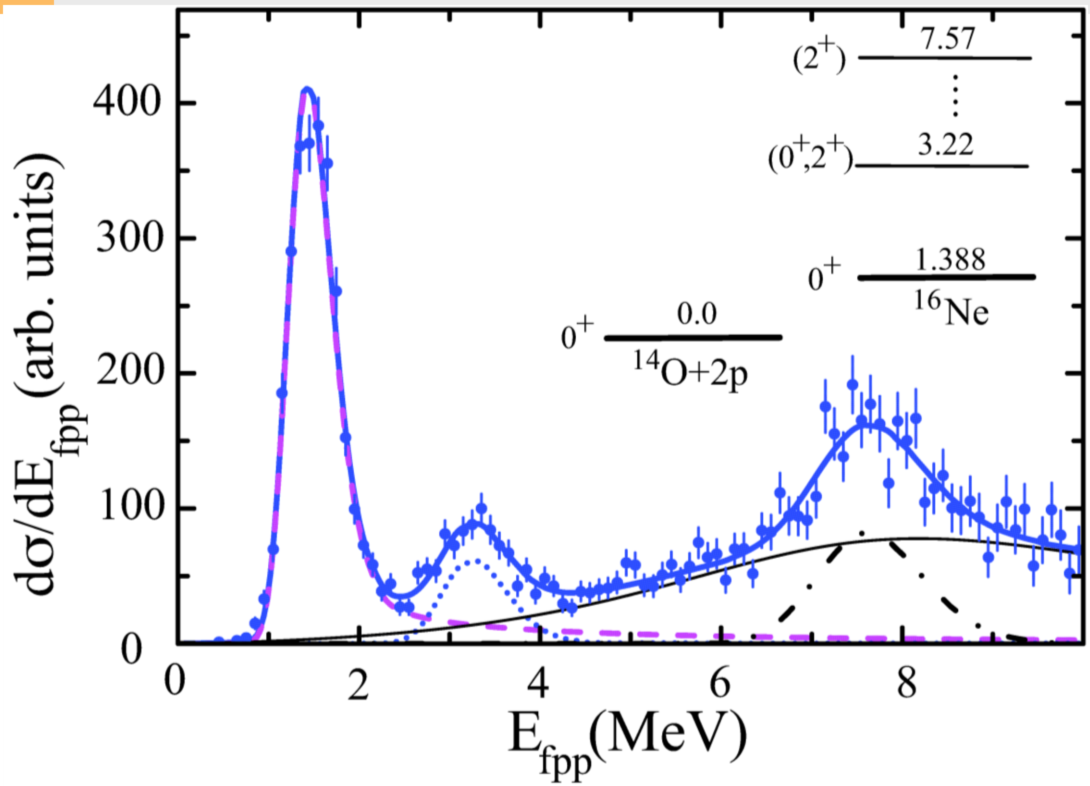

$I^\pi = 0^+$		$I^\pi = (0^+,2^+)$		$I^\pi = (2^+)$		
E_r	Γ	E_r	Γ	E_r	Γ	Ref.
1.388(15)	0.082(15)	3.22(5)	≤ 0.05	7.57(6)	≤ 0.1	[⋆]
1.33(8)	0.2(1)	3.02(11)	–	–	–	[11]
1.466(45)	–	–	–	–	–	[12]
1.399(24)	0.11(4)	–	–	–	–	[13]
–	–	3.5(2)	–	–	–	[14]
1.35(8)	–	–	–	7.6(2)	$0.8(^{+4}_{-8})$	[15]

[11] G.J. KeKelis et al., Phys. Rev. C 17, 1929 (1978).
[12] G.R. Burleson et al., Phys. Rev. C 22, 1180 (1980).
[13] C.J. Woodward, R.E. Tribble and D.M. Tanner, Phys. Rev. C 27, 27 (1983).
[14] K. Föhl et al., Phys. Rev. Lett. 79, 3849 (1997).
[15] I. Mukha et al., Phys. Rev. C 79, 061301(R) (2009)

Confirmation of previous results.
Narrow width for
1st and 2nd excited state.

K.W. Brown et al,
Phys.Rev.Lett. 113, 232501 (2014)
gs. Er=1.476(20) Γ<60keV
„width puzzle“

^{15}Ne Mass: prediction via mirror nuclei systematics

F. Wamers et al., PRL 112, 132502 (2014)

„Improved Garvey-Kelson Mass relations" (sytematics) *J. Tian et al, Phys. Rev. **C 87,** 014313 (2013)*

→ ME(^{15}Ne) = 41.555(23) MeV, vs. ME(^{15}Ne)$_{exp}$ = 40.215(69) MeV

Model: N,Z=8,10 (sd)^2 shell nuclei: |g.s.> ~ $\alpha(1s_{1/2})^2 + \beta(0d_{5/2})^2$ | P(s²)=66(10)%, ^{16}C-^{15}**B**-^{14}Be

→ ME(^{15}Ne) = 40.37(24) MeV, vs ME(^{15}Ne)$_{exp}$ = 40.215(69) MeV

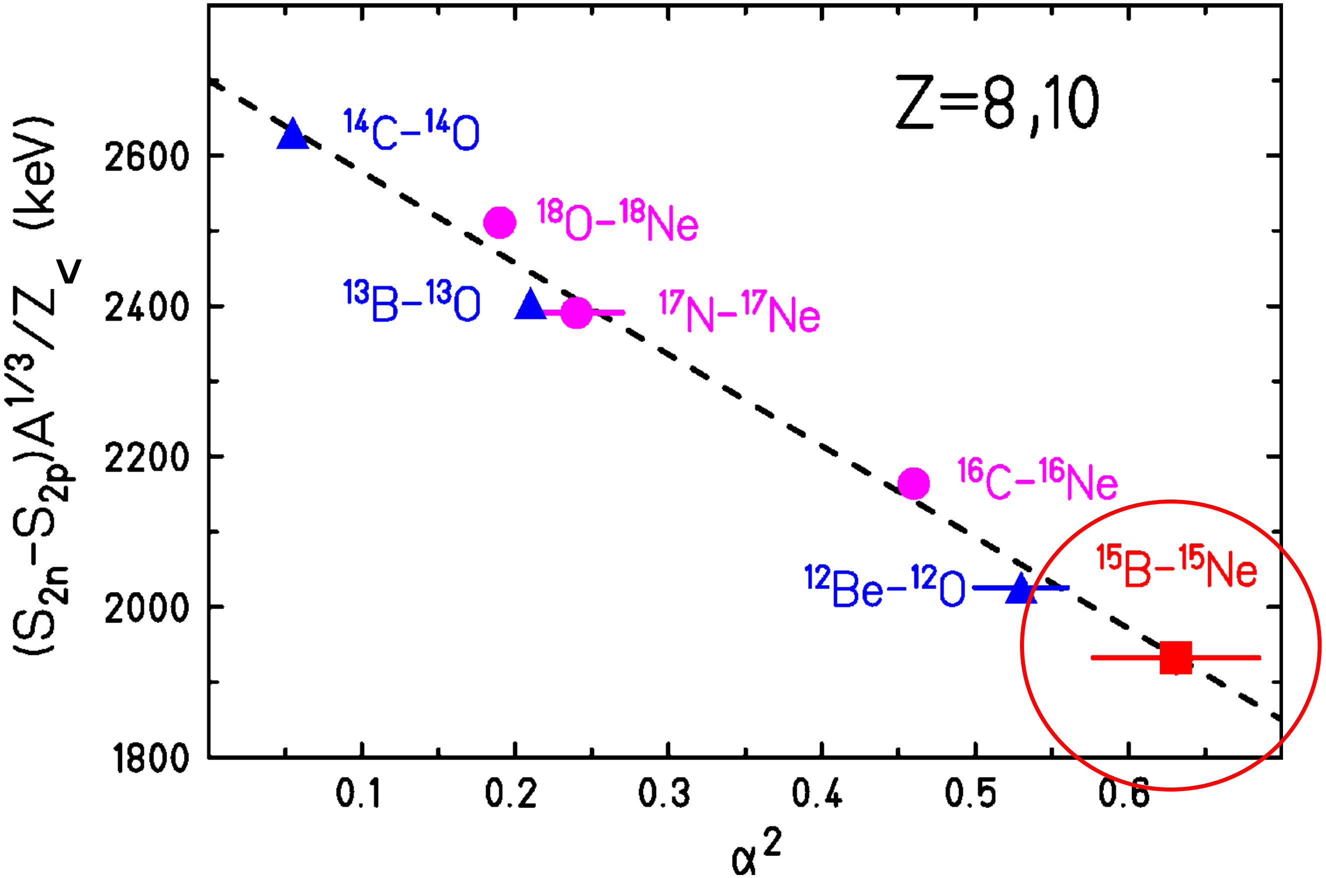

*H.T. Fortune, Phys. Lett. **B718**, 1342 (2013)*

→ 63(5) % of $(1s_{1/2})^2$ in ^{15}Ne ground state

NeuLAND:
The High Resolution Neutron Time-of-Flight Spectrometer for R^3B

K. Boretzky

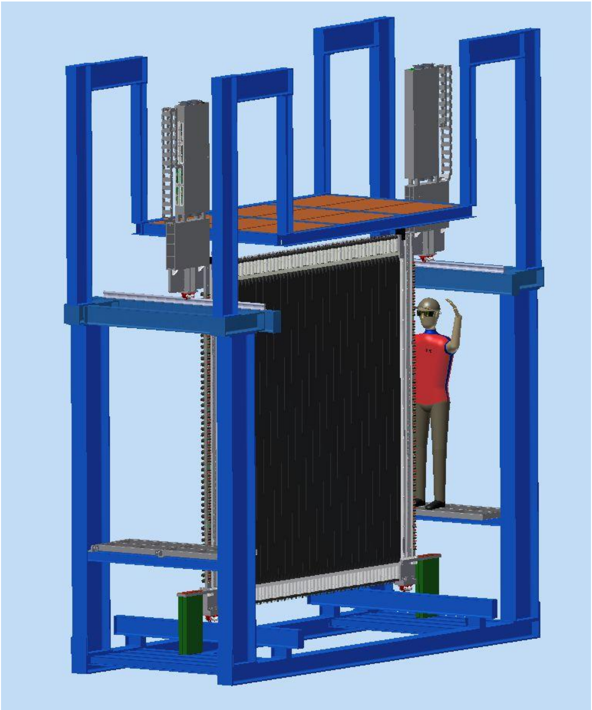

NeuLAND detector parameters:

- full active detector using RP/BC408
- face sice 250x250 cm^2
- active depth 300 cm
- 3000 scintillator bars
- 6000 PM / readout channels
- 32 tons

NeuLAND design goals:

- **>**90% efficiency for 0.2-1.0 GeV neutrons
- Multi-hit capability for up to 5 neutrons
- invariant-mass resolution: **NeuLAND-target distance 35 m**

  ΔE < 20 keV at 100 keV above the neutron threshold

Going Neutron rich …

P.G. Hansen, Nature 328 (1987) 476

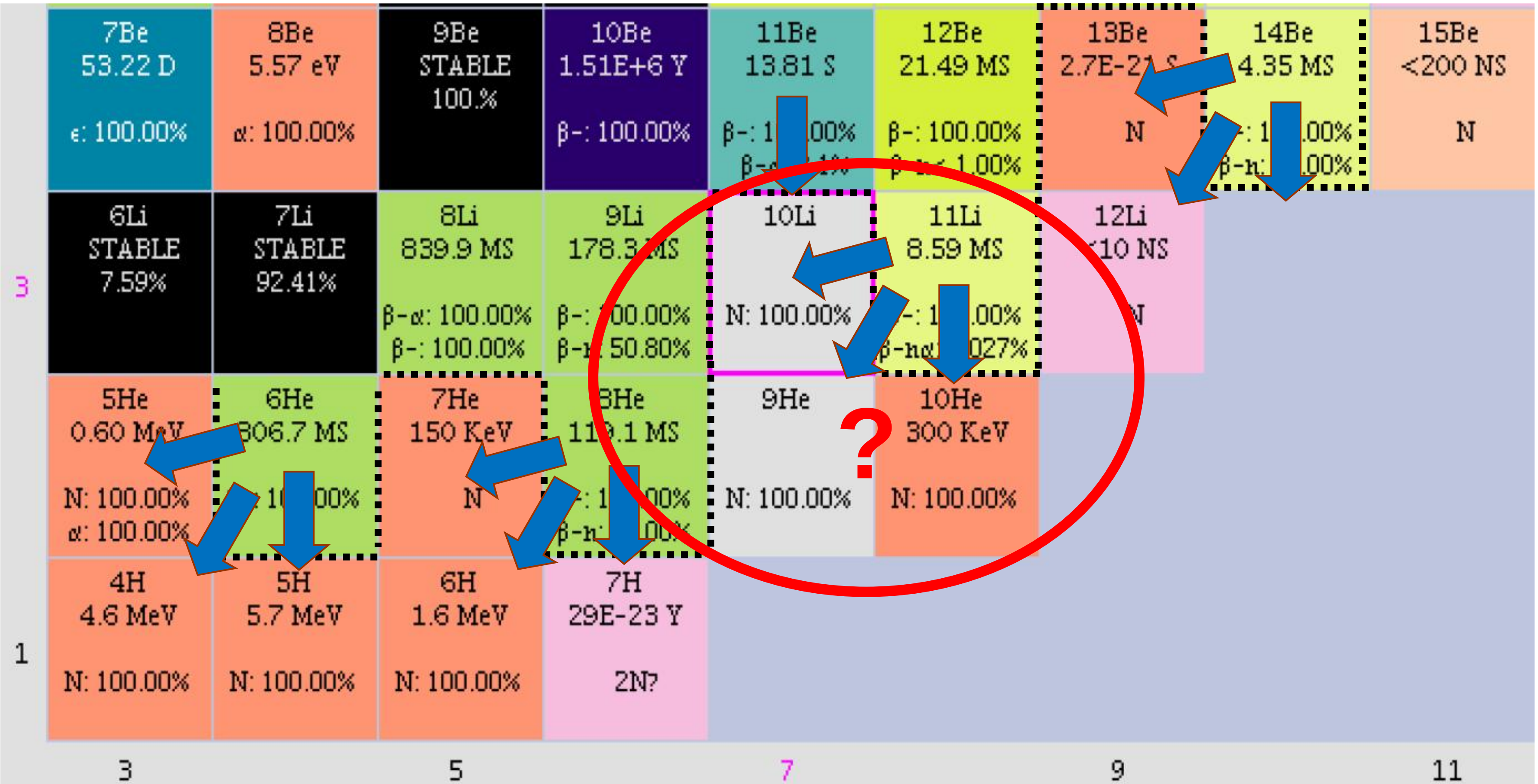

[11]Li with „known“ structure ➔ initial vs. final state

Influence of reaction mechanism ➔ different seed nuclei